Plasmodium DDI1 is an essential chromatin-associated protein with a role in DNA-protein crosslink repair

Nandita Tanneru[1,#], M Angel Nivya[1,#], Navin Adhikari[1,#], Kanika Saxena[1,2], Zeba Rizvi[1], Renu Sudhakar[1], Amit Kumar Nagwani[1], Atul[1], Faisal Mohammed Abdul Al-Nihmi[3], Kota Arun Kumar[3], Puran Singh Sijwali[1,2*]

[1]CSIR-Centre for Cellular and Molecular Biology, Hyderabad-500007, TS, India

[2]Academy of Scientific and Innovative Research, Ghaziabad-201002, UP, India

[3]Department of Animal Biology, School of Life Sciences, University of Hyderabad, Hyderabad 500046, India

[#]These authors made equal contribution to the study

[*]Corresponding author: Puran Singh Sijwali, Email: psijwali@ccmb.res.in

Keywords: DNA damage inducible 1 protein, retroviral aspartyl protease, DPC, malaria, HIV protease inhibitor, ubiquitin proteasome system

Running title: Plasmodium DDI1 contributes to DPC repair

ABSTRACT

DDI1 proteins are conserved in eukaryotes and involved in a variety of cellular processes, including proteasomal degradation of specific proteins and DNA-protein crosslink repair. All DDI1 proteins contain ubiquitin-like (UBL) and retroviral aspartyl protease (RVP) domains, and some also contain ubiquitin-associated (UBA) domain, which mediate distinct activities of these proteins. We investigated the *Plasmodium* DDI1 to identify its roles during parasite development and potential as a therapeutic target. The DDI1 proteins of *Plasmodium* and other Apicomplexan parasites vary in domain architecture, share UBL and RVP domains, and the majority of proteins contain the UBA domain. *Plasmodium* DDI1 is expressed across all major life stages and is essential, as conditional depletion of DDI1 protein in *P. berghei* and *P. falciparum* drastically reduced the asexual stage parasite development. Infection of mice with DDI1 knock-down *P. berghei* parasites was self-limiting and protected from the subsequent infection with both homologous and heterologous parasites, indicating potential of DDI1 knock-down parasites as a whole organism vaccine. *P. falciparum* DDI1 (PfDDI1) is associated with chromatin and DNA-protein crosslinks, and PfDDI1 knock-down parasites showed increased DNA-protein crosslinks and susceptibility to DNA damaging chemicals, indicating an important role for DDI1 in repair of DNA-protein crosslinks. The knock-down of PfDDI1 increased susceptibility to retroviral protease inhibitors, epoxomicin and artemisinin, which suggests that simultaneous inhibition of DDI1 could potentiate antimalarial activity of these inhibitors or drugs. Hence, the essentiality, ability of DDI1 knock-down parasites to confer protective immunity and increased susceptibility to inhibitors support *Plasmodium* DDI1 as a dual-target therapeutic candidate.

INTRODUCTION

The ubiquitin proteasome system (UPS) is a major degradation machinery for clearance of unwanted and misfolded proteins in eukaryotes, which is vital for maintaining cellular homeostasis (1, 2). Proteasome inhibitors have been shown to block the development of malaria parasites at multiple stages, indicating a critical role of the UPS during parasite development (3-5). Hence, the proteasome of protozoan parasites, including *Plasmodium*, has emerged as a potential drug target (6-9). The UPS includes ubiquitin, enzymes involved in tagging the substrate with ubiquitin and the 26S proteasome wherein ubiquitinated proteins are degraded (10, 11). Several non-proteasomal ubiquitin-binding proteins also contribute to the proteasome function. One such class of proteins are the shuttle proteins, which include Rad23, Dsk2 and DDI1 (12, 13). These proteins contain a ubiquitin-like (UBL) domain and a ubiquitin-associated (UBA) domain, which mediate their interactions with the proteasome and ubiquitin chains of the ubiquitinated protein, respectively. DDI1 also contains an aspartyl protease domain similar to the retroviral aspartic protease (RVP) of HIV protease (14).

DDI1 was first discovered as one of the over expressed proteins upon treatment of *Saccharomyces cerevisiae* with DNA damaging agents, hence, it was named as the DNA damage inducible 1 protein (DDI1) (15). A later study named it v-SNARE master 1 (VSM1) based on its interaction with Snc2 v-SNARE proteins, and showed that knockout of VSM1 increased protein secretion (16). VSM1/DDI1 inhibits assembly of Sso t-SNAREs with Sec9 t-SNARE, which is required for exocytosis (17, 18). Deletion analysis demonstrated that both UBL and RVP domains of *S. cerevisiae* DDI1 (ScDDI1) are necessary for inhibition of protein secretion. However, the ScDDI1 C-terminal that contains the Sso t-SNARE-binding region and UBA domain was found to be dispensable for suppression of protein secretion (19), which indicated that suppression of protein secretion by VSM1/DDI1 is independent of its interaction with Sso t-SNARE. Over expression of ScDDI1 rescued the S-phase checkpoint defect of a temperature sensitive Pds1 mutant, which required the UBA but not UBL domain (20). Another study showed that UBL, catalytically competent RVP and UBA domains of ScDDI1 are required for the rescue of S-phase checkpoint defect (18). ScDDI1 has been shown to shuttle ubiquitinated Ho endonuclease to the proteasome for degradation, which requires interaction of UBA and UBL domains with ubiquitinated Ho endonuclease and the Rpn1 subunit of 26S proteasome, respectively (21, 22).

Interaction of the ScDDI1 UBL domain with the ubiquitin interaction motif (UIM) of the F-box protein Ufo1 has been shown to be critical for proteasomal degradation of Ufo1 (23). The UBA domain of ScDDI1 homolog in *Schizosaccharomyces pombe*, Mud1, has also been shown to bind Lys48-linked polyubiquitin chains (24). Interestingly, DDI1 itself is a substrate of E3 ligase UBE3A in *Drosophila melanogaster*, which does not target ubiquitinated DDI1 for degradation, and the biological significance of ubiquitination of DDI1 is not known yet (25). Recent studies have demonstrated important roles of ScDDI1 in repair of DNA-protein crosslinks (DPC) and alleviation of DNA replication stress caused by hydroxyurea (26, 27). Both these functions require catalytically competent ScDDI1, indicating that ScDDI1 functions as a protease.

The DDI1 homolog of *Drosophila melanogaster*, Rngo, is essential for oocyte formation (28). As has been shown for ScDDI1, Rngo has been shown to dimerize through the RVP domain, binds ubiquitin via the UBA domain and interacts with the Rpn10 subunit of the proteasome via the UBL domain. The *Homo sapiens* DDI2 (HsDDI2) and *Caenorhabditis elegans* DDI1 (CeDDI1) have been shown to cleave the ER-associated Nrf1/Skn-1A, which results in the release and translocation of the cleaved form to the nucleus wherein it upregulates the proteasome genes (29, 30). Despite multiple studies indicating requirement of catalytically competent DDI1, a direct demonstration of the protease activity of DDI1 proteins has been elusive until recently. Two recent studies directly demonstrated that HsDDI2 and ScDDI1 cleave ubiquitinated Nrf1 and a peptide substrate corresponding to the Nrf1 cleavage site, respectively (31, 32). These two studies also indicated that ScDDI1 and HsDDI2 do not cleave the ubiquitin chains, hence, unlikely to function as deubiquitinases.

As described above, multiple studies highlight contributions of UBL, RVP and UBA domains in functions of DDI1 proteins. How these domains crosstalk with each other in the full-length DDI1 is not known due to the unavailability of a full-length DDI1 structure. Structural studies of the RVP domains of ScDDI1, LmDDI1 and human DDI2 revealed that RVP domain exists as a dimer in which aspartyl protease motifs from both the monomers contribute to the formation of active site (14, 33-35). The active site of ScDDI1 has identical geometry with that of HIV protease, but has wider substrate binding groove than HIV protease, suggesting that ScDDI1 can accommodate bulkier substrates (14). Interestingly, in addition to the UBA domain, the UBL

domains of ScDDI1 and HsDDI2 also contain a ubiquitin-interaction motif (UIM) that mediates interaction with ubiquitin (33, 34, 36).

As a therapeutic target, not much is explored on the role of DDI1 in many economically important protozoan parasites, despite a significant adverse impact of these on human and domestic animal health. The DDI1 proteins of *Leishmania major* and *Toxoplasma gondii* are the only reported representatives. The *Leishmania major* DDI1 (LmDDI1) has been proposed to be the major target of the anti-leishmanial effect of HIV protease inhibitors (37). Recombinant LmDDI1 has also been shown to degrade peptides and BSA at pH 4-5, which appears to be contrary to the presence of DDI1 proteins in cytosolic pH environment (38). Knock-out of *Toxoplasma gondii* DDI1 (TgDDI1) has been shown to cause accumulation of ubiquitinated proteins and loss of virulence (39). HIV protease inhibitors have been shown to block the development of malaria parasites at multiple stages (40-44). Furthermore, a study in humans showed that treatment with HIV protease inhibitor-based antiretroviral therapy reduced incidence of malaria by 41% compared to the group treated with non-protease inhibitor-based anti-retroviral therapy, and the lower incidence was attributable to decreased recurrence of malaria (45). As DDI1 is important for several cellular processes and the presence of RVP domain makes it a potential target of HIV protease inhibitors, we undertook cellular, genetic and biochemical approaches to investigate the *Plasmodium* DDI1. Our study revealed that *Plasmodium* DDI1 is essential for parasite development, associated with chromatin and contributes to DPC repair, and it could be a target of HIV protease inhibitors.

RESULTS

DDI1 proteins of apicomplexan parasites exhibit diverse domain organizations. *S. cerevisiae* DDD1 (ScDDI1) is the most studied among all DDI1 proteins, and we used it as a query sequence to search the *P. falciparum* genome database (PlasmoDB). A protein encoded by the PF3D7_1409300 gene and annotated as "DNA damage-inducible protein 1, putative" came out as the closest homolog. This protein was termed as the *P. falciparum* DNA damage-inducible protein 1 (PfDDI1), as it shares 33% identity with ScDDI1, contains putative UBL and RVP domains, and has a putative aspartyl protease motif (FVDSGA) in the RVP domain (Figure 1). Canonical aspartyl proteases like pepsin contain two copies of the catalytic motif "VFDTGS" (Xaa-Xaa-Asp-Xbb-Gly-Xcc, where Xaa is a hydrophobic residue, Xbb is Thr or Ser, and Xcc is Ser), which together form the active site. The HIV aspartyl protease or retroviral aspartyl proteases possess a single catalytic motif (LLDTGA in HIV protease), hence, exists as a dimer in which the catalytic motif of both the monomers form the active site (46). DDI1 proteins, including PfDDI1, contain a single catalytic motif (Figure 1). The X-ray crystal structures of RVP domains of ScDDI1, HsDDI2 and LmDDI1 indicate that they exist as dimers in which catalytic motifs of both the monomers form the active site (14, 33, 35). Since a full-length DDI1 structure is not available yet, we compared the AlphaFold structure of full-length PfDDI1 (AF-Q8IM03-F1) with ScDDI1 UBL and RVP domains (PDB IDs: 2N7E for ScDDI1 UBL, 2I1A for ScDDI1 RVP), which were found to be comparable (RMSD: 1.165 for UBL and 0.544 for RVP domains; Figure S1) and supported the multi-domain architecture of PfDDI1.

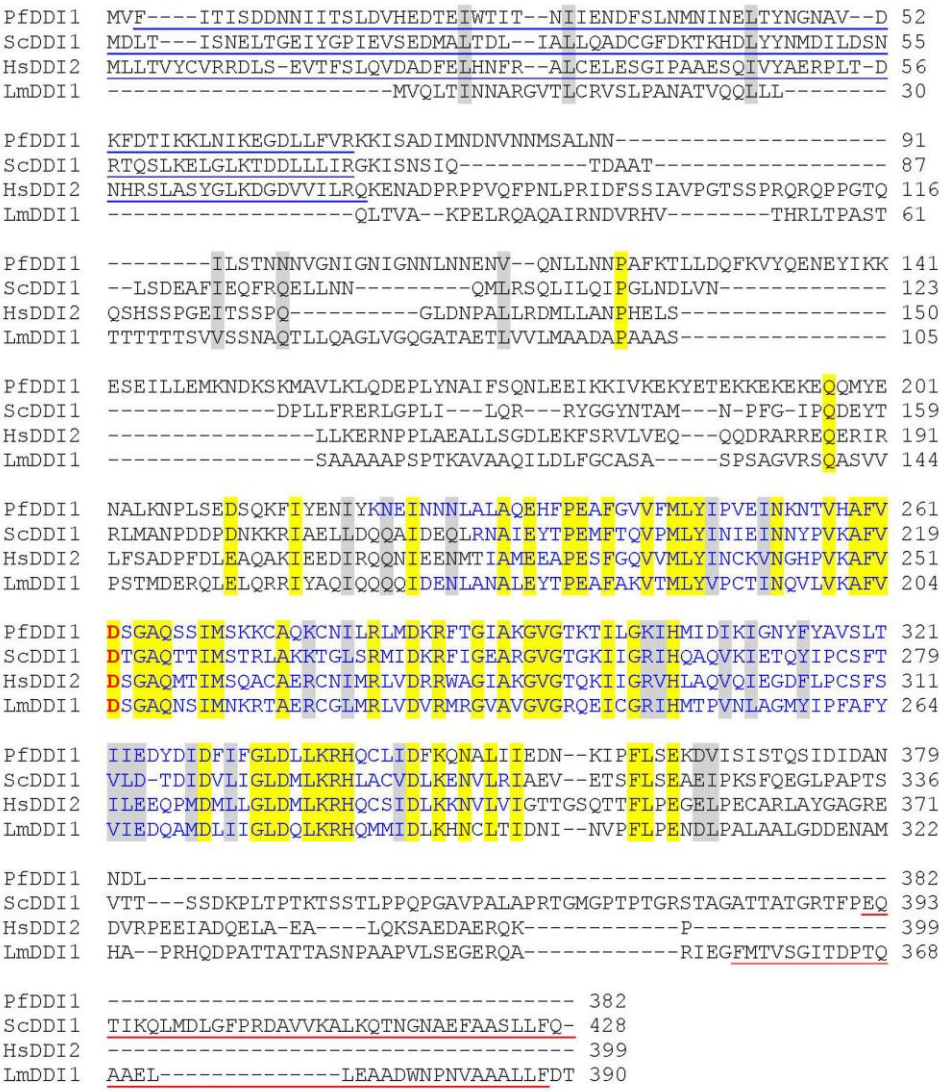

Figure 1. Sequence alignment of DDI1 proteins. The amino acid sequence of *P. falciparum* DDI1 (PfDDI1) was aligned with the sequences of structurally characterized orthologs from *S. cerevisiae* (ScDDI1) and *H. sapience* (HsDDI2) and *L. major* (LmDDI1). The UBL domain is marked with a blue line, RVP domain is in blue font and UBA domain is marked with a red line. Conserved amino acid residues are highlighted in yellow and physico-chemically similar residues are highlighted in grey. The number at the end of each line indicate the position of the last amino acid residue in the respective protein. The predicted catalytic aspartate residue is in red font.

Plasmodium species encode for a single DDI1 ortholog, which have the same domain architecture and are 69-94% identical at amino acid level. The apicomplexan parasites sequenced to date also encode a single DDI1 ortholog, which vary in size, sequence and domain architecture. The catalytic motif in the majority of apicomplexan DDI1 proteins is "FVDSGA", whereas it is "LVDTGA" in *Theileria*, *Cytauxzoon* and the majority of *Babesia* species. Interestingly, *Babesia microti* contains "FVDTGA", which is a chimera of "FVDSGA" and "LVDTGA". Analysis of the

Apicomplexan DDI1 protein sequences for conserved domains and structurally similar domains revealed diversity in their domain architectures (Figure 2A). All Apicomplexan DDI1 proteins contain the UBL and RVP domains. DDI1 proteins of the parasites of Sarcocystidae (*Besnoitia, Cystoisospora, Hammondia, Neospora, Sarcocystis* and *Toxoplasma*), Cryptosporidiidae (*Cryptosporidium*) and Theileriidae (*Theileria* and *Cytauxzoon*) families also contain the UBA domain. The DDI1 proteins of Babesiidae parasites contain all three domains (*Babesia microti*), UBL and RVP domains (*Babesia bovis*) or DUF676, UBL and RVP domains (*Babesia divergens* and *Babesia bigemina*). The sizes of Apicomplexan DDI1 proteins vary from 275 amino acid residues (*Gregarina niphandrodes*) to 1191 amino acid residues (*Babesia bigemina*). We also performed homology modelling of the representative DDI1 proteins listed in Figure 2 (data not shown), which was consistent with the conserved domain analysis-based prediction. Homology modelling predicted UBL domain in *Gregarina niphandrodes* DDI1, and UBA domains in *Theileria annulata* and *Cytauxzoon felis* DDI1 proteins (Figure S1), which could not be predicted using the conserved domain analysis. The diversity in domain architecture may impart species-specific functions or regulation of DDI1 proteins in Apicomplexan parasites. The Apicomplexan DDI1 proteins clustered on different branches in a phylogenetic tree (Figure 2B), indicating sequence diversity across the Apicomplexa phylum. Nonetheless, the phylogram reflected evolutionary relatedness of different parasites, as DDI1 proteins of the same family clustered on the same branch and those of the same order shared the root. For example, parasites of the families Babesiidae and Theileriidae in the order Piroplasmida shared a common root.

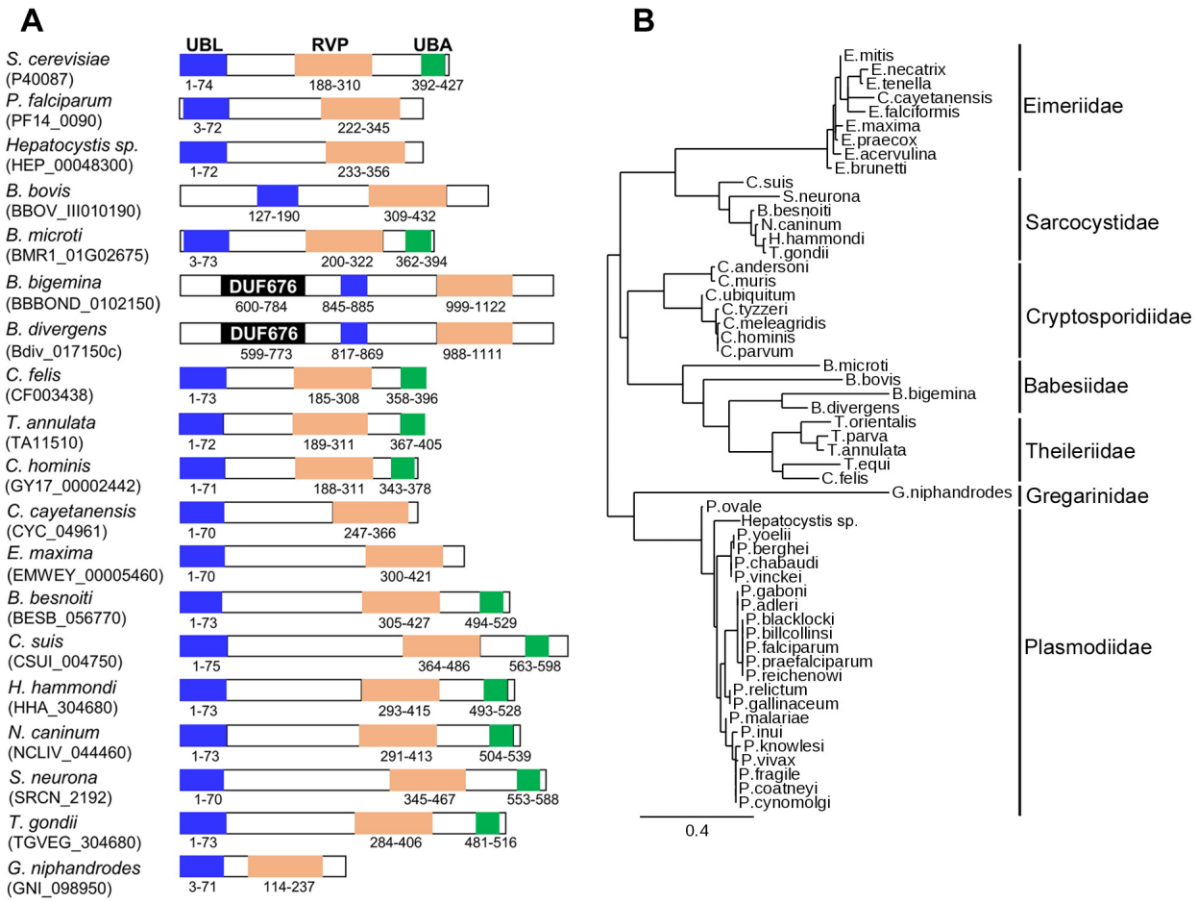

Figure 2. Domain organization and phylogenetic relatedness of DDI1 proteins. A. Sequences of the DDI1 proteins of indicated Apicomplexan parasites were analyzed for the presence of conserved domains and compared with the *S. cerevisiae* DDI1 domain architecture. The location and position of boundary amino acids of UBL, RVP and UBA domains are shown. The length of each schematic is sized according to the length of respective DDI1 protein except for *B. bigemina* and *B. divergens*. **B.** The sequences of 54 DDI1 proteins of the indicated parasite species of different families were used for generation of the phylogram.

***Plasmodium* DDI1 is expressed in all major parasite stages.** The full-length PfDDI1 coding region was expressed as an N-terminal His-tagged protein in M15(pREP4) cells using the pQE30 vector, purified under denaturing conditions, refolded and used for antibody generation in rats (Figure S2). The antiserum was adsorbed on M15(pREP4) cells to remove cross-reactive antibodies to *E. coli* proteins, and the adsorbed PfDDI1 antiserum was used to determine the expression and localization of PfDDI1 in different parasite stages. The PfDDI1 antiserum detected a prominent band of the size of full-length PfDDI1 (~43.8 kDa) in the western of *P. falciparum* ring, trophozoite and schizont stages (Figure 3), confirming expression in these stages. For cellular localization, we performed immunofluorescence assay (IFA) of *P. falciparum* erythrocytic and

gametocyte stages with PfDDI1 antiserum, which indicated expression of PfDDI1 in both asexual and sexual stages (Figure 3 and 4). To check if DDI1 is expressed in insect and liver stages, we turned to *P. berghei*, which offers studies in insect and liver stages with ease compared to *P. falciparum*. As PfDDI1 and *P. berghei* DDI1 (PbDDI1) share 70.5% identity, PfDDI1 antiserum detected PbDDI1 in the western blot and showed prominent signal in the IFA of trophozoite, sporozoite and liver stage schizont of *P. berghei* (Figure 5), which indicated expression of PbDDI1 in these stages. In addition to the full-length PfDDI1, we also observed smaller size band in the western blots, which could be the processed form of full-length protein. The western blot and IFA data of *P. falciparum* and *P. berghei* DDI1 proteins together indicate that *Plasmodium* DDI1 is expressed in all major development stages of malaria parasites.

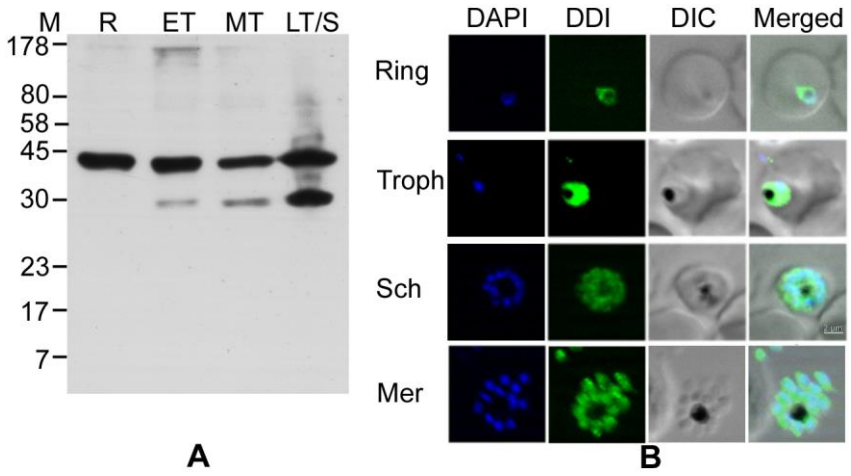

Figure 3. Expression and localization of PfDDI1 in asexual erythrocytic stages. A synchronized culture of *P. falciparum* was harvested at different stages for expression and localization of PfDDI1. **A.** The western blot of lysates of ring (R), early trophozoite (ET), mid trophozoite (MT) and late trophozoite/schiziont (LT/S) stage parasites was probed using PfDDI1 antiserum. Protein size markers are in kDa (M). **B**. Ring, trophozoite (Troph), schizont (Sch) and free merozoite (Mer) stages were assessed for localization of by IFA using PfDDI1 antiserum. The panels show nucleic acid staining (DAPI), PfDDI1 signal (DDI), bright field with RBC and parasite boundaries (DIC) and the overlap of all three images (Merged). The black substance is haemozoin, a food vacuole-resident pigment.

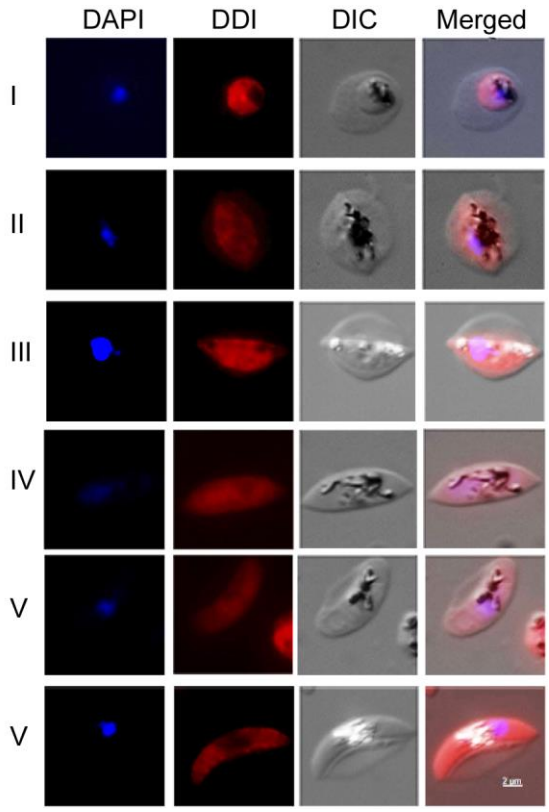

Figure 4. Localization of PfDDI1 in sexual erythrocytic stages. The indicated gametocyte stages of *P. falciparum* were evaluated for expression of PfDDI1 by IFA using PfDDI1 antiserum. The panels show nucleic acid staining (DAPI), PfDDI1 signal (DDI), bright field with RBC and parasite boundaries (DIC) and the overlap of all three images (Merged). The black substance is the food vacuole-resident pigment haemozoin.

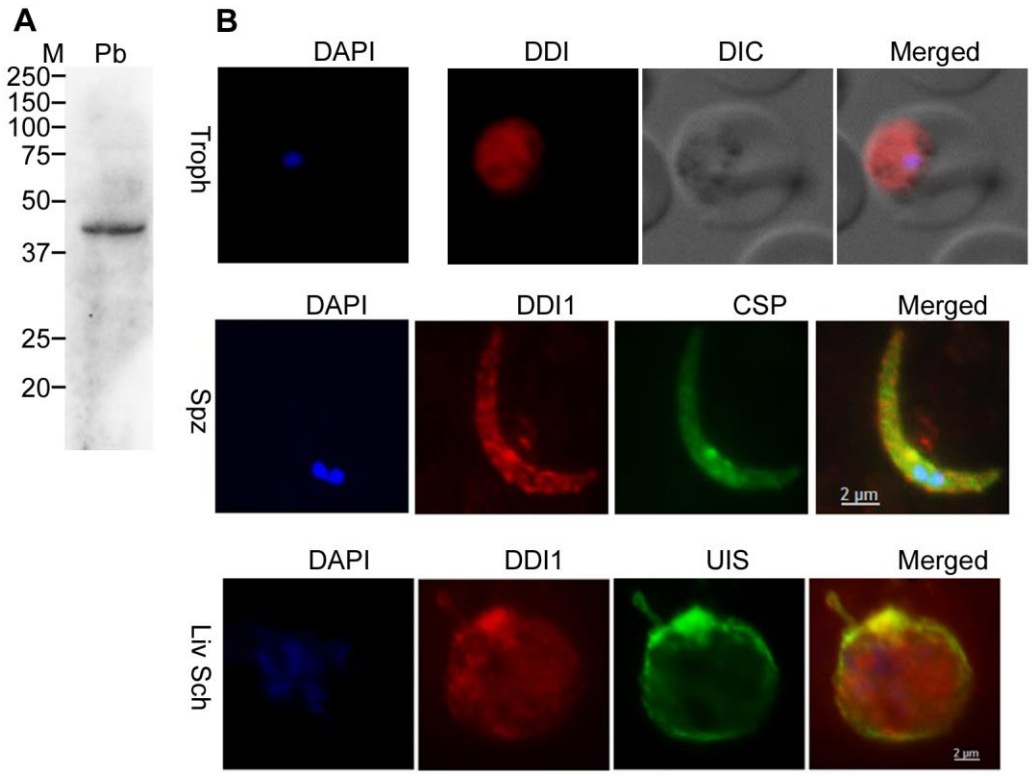

Figure 5. Expression and localization of PbDDI1. A. The western blot of *P. berghei* asexual erythrocytic stage parasites was probed using PfDDI1 antiserum to check for PbDDI1 expression. The prominent signal corresponds to the predicted size of native PbDDI1 (~44.3 kDa). Protein size markers are in kDa (M). **B.** *P. berghei* erythrocytic trophozoite (Troph), sporozoite (Spz) and liver schizont (Liv Sch) stages were evaluated for localization of PbDDI1 by IFA using PfDDI1 antiserum along with antibodies to CSP (a sporozoite membrane marker) and UIS (a liver stage parasitophorous vacuole marker). The panels are for nucleic acid staining (DAPI), PbDDI1 signal (DDI), signal for CSP and UIS, bright field with RBC and parasite boundaries (DIC), and the overlap of three images (Merged).

DDI1 is essential for parasite development. Expression of DDI1 in all the major parasite stages suggests its importance for parasite development. Hence, we attempted to knock-out the PbDDI1 gene for investigation of its functions during parasite development. However, multiple knock-out attempts were unsuccessful. We next employed a conditional knock-down approach in *P. berghei* by replacing the wild type PbDDI1 coding region with $PfDDI_{Myc}/cDD_{HA}$ coding sequence, which would express fusion of $PfDDI_{Myc}$ with HA-tagged mutant *E. coli* DHFR (cDD_{HA}). cDD binds trimethoprim and is stable, but undergoes proteasomal degradation in the absence of trimethoprim, thereby, causing a knock-down effect. The replacement of wild type PbDDI1 with $PfDDI_{Myc}/cDD_{HA}$ and expression of DDI_{Myc}/cDD_{HA} fusion protein were successful (Figure S3), which confirmed that PbDDI1 and PfDDI1 are functionally conserved. The knock-down parasites (PbKD) showed reduction in DDI_{Myc}/cDD_{HA} protein level in the absence of trimethoprim

compared to that in the presence of trimethoprim, indicating the knock-down effect (Figure 6A). PbKD parasites grew similar to wild type parasites in the presence of trimethoprim, but showed drastically reduced growth in the absence of trimethoprim and eventually disappeared (Figure 6B). In the presence of trimethoprim, PbKD-infected mice had to be euthanized, whereas in the absence of trimethoprim, the parasitemia barely reached to 0.5% and the infection was self-limiting. Withdrawal of trimethoprim from PbKD-infected mice at about 5% parasitemia also resulted in complete clearance of parasites (Figure 6C).

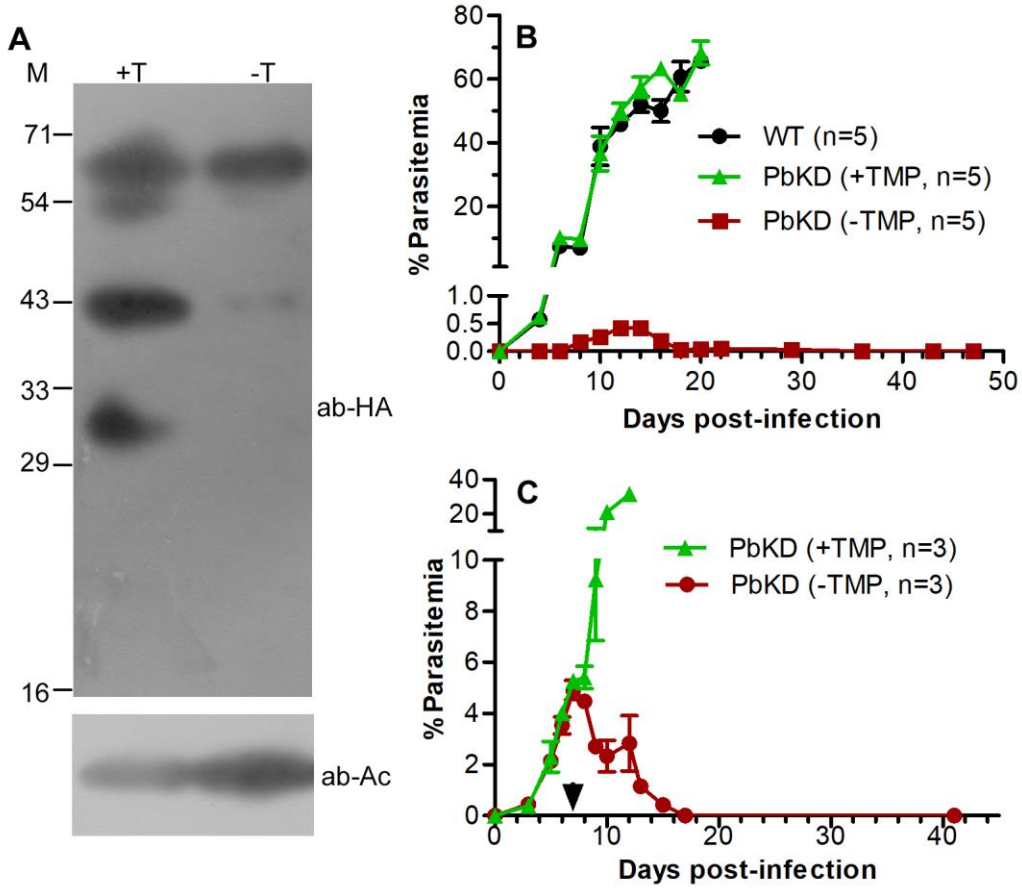

Figure 6. DDI1 is critical for *P. berghei* development. A. DDI1 knock-down *P. berghei* parasites (PbKD) were cultured in the presence (+T) or absence (-T) of trimethoprim, and parasite lysates were assessed for DDI_{Myc}/cDD_{HA} protein level by western blotting using antibodies to HA (ab-HA) and β-actin (ab-Ac) as a loading control. The top band corresponds to the predicted size of full-length protein (~64.4 kDa) and the sizes of protein markers are in kDa (M). **B.** Mice were infected with equal number of wild type *P. berghei* ANKA (WT) or PbKD parasites and infection was monitored. The mice infected with PbKD were kept under (+TMP) or without (-TMP) trimethoprim. The number of mice in each group is shown with "n", and parasite growth is shown as % parasitemia over days post-infection. **C.** Mice were infected with PbKD and kept under trimethoprim until 5% parasitemia. Trimethoprim was withdrawn from one group of mice (-TMP), whereas the other group was maintained under trimethoprim (+TMP). Infection was monitored, "n" is the number of mice in each group, and parasite growth is shown as % parasitemia over days post-infection.

We similarly generated a *P. falciparum* line expressing $PfDDI_{Myc}/cDD_{HA}$ in place of the wild type PfDDI1, and assessed the knock-down parasites (PfKD) for various parameters, including the parasite development. PfKD parasites showed successful gene replacement and expression of DDI_{Myc}/cDD_{HA} fusion protein (Figure S4). The PfKD parasites grown in the absence of trimethoprim showed decreased DDI_{Myc}/cDD_{HA} protein level and growth as compared to those grown in the presence of trimethoprim (Figure 7), indicating that DDI1 is important for asexual erythrocytic stage parasite development of *P. falciparum* as well. The knock-down effect was more prominent both as reduction in protein level and growth with increased period of growth without trimethoprim. Failure to knock-out PbDD1, drastically decreased growth and loss of virulence of PbKD parasites, and decreased growth of PfKD parasites support an essential role of DDI1 during asexual stage parasite development.

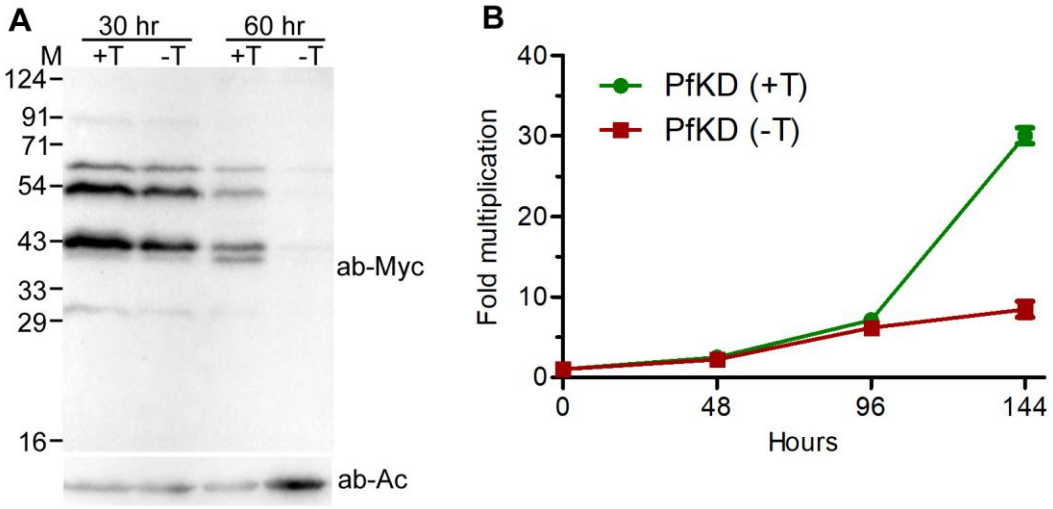

Figure 7. Knock-down of DDI1 in *P. falciparum* drastically reduced parasite growth. A. Synchronized ring stage PfKD parasites were cultured in the presence (+T) or absence (-T) of trimethoprim, harvested at 30 hour and 60 hour stages of development, and processed for western blotting using antibodies to Myc (ab-Myc) and β-actin (ab-Ac) as a loading control. The top band corresponds to the predicted size of full-length protein (~64.4 kDa). **B.** PfKD parasites were cultured with (+T) or without (-T) trimethoprim for three consecutive cycles. Parasitemia was determined at the beginning and end of each cycle, normalized to the initial parasitemia, and shown as fold multiplication over growth cycles. The data is mean of two independent experiments with SD error bar.

Prior infection of mice with PbKD parasites protects from subsequent infection. Since mice infected with PbKD parasite resolved infection in the absence of trimethoprim, we assessed if the

recovered mice developed immunity. Groups of naïve and recovered mice were challenged with a lethal inoculum of wild type *P. berghei* ANKA and infection was monitored. The naïve mice developed high parasitemia and succumbed to infection, whereas the recovered mice either did not develop infection or cleared infection after developing a low level of parasitemia (Figure 8). This indicated that prior exposure of mice to PbKD parasites conferred protective immunity. The recovered mice also showed protection against a lethal *P. yoelii* 17XNL challenge (Figure 8), which indicated that prior exposure of mice with PbKD parasites protects from a heterologous challenge as well. The pooled serum, which was collected from the recovered mice one day before the challenge, showed reactivity with soluble parasite extract in ELISA, with a titer as high as 1/128000, suggesting that anti-parasite antibodies could have contributed to protection from the subsequent parasite challenge.

Owing to the essentiality of PbDDI1 and its prominent expression in blood stages, we produced recombinant PbDDI1 (Figure S5), immunized mice with it and challenged the mice with wild type *P. berghei* ANKA. The mice immunized with recombinant PbDDI1 developed high antibody titer against recombinant PbDDI1 (ELISA antibody titer: 1/600000), but showed infection just like naïve and adjuvant control mice (Figure 8). This ruled out PbDDI1 as a natural target of immune response, and indicated that prior infection of mice with PbKD parasites elicits a protective immune response, most likely against the whole parasite.

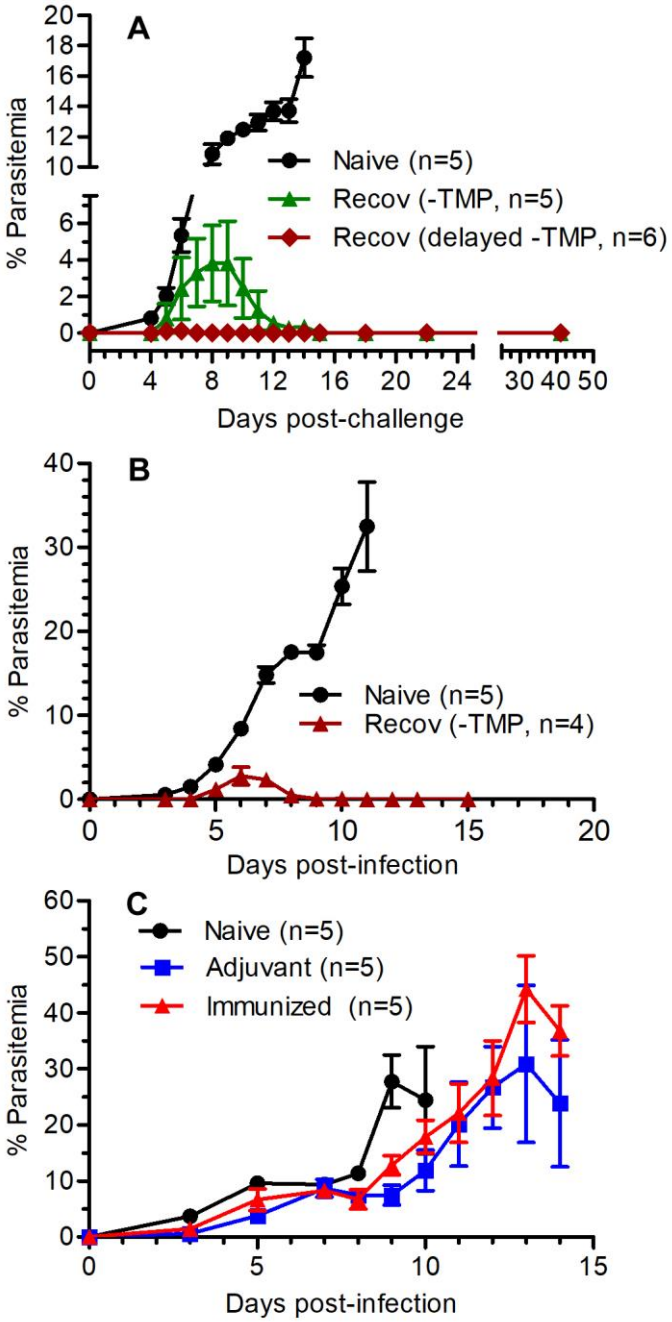

Figure 8. Prior infection of mice with PbKD parasites elicits protective immunity. A. The naïve and recovered mice were challenged with equal number of wild type *P. berghei* ANKA, infection was monitored and shown as % parasitemia over days post-infection. The recovered group that was never given trimethoprim during PbKD parasite infection is indicated with "Recov (-TMP)" and those mice that recovered from PbKD infection after late withdrawal of trimethoprim are indicated with "Recov (delayed –TMP)". **B.** Naïve and recovered (Recov) mice were infected with equal number of *P. yoelii* 17XNL parasites, infection was monitored and shown as % parasitemia over days post-infection. C. Mice were immunized with recombinant PbDDI1+adjuvant (immunized), adjuvant only (adjuvant) or left without immunization (naïve). All the three groups of mice were challenged with equal number of *P. berghei* ANKA parasites, infection was monitored and shown as % parasitemia over days post-infection. For all three plots, "n" represents the number of mice and each data point represents the mean of % parasitemias of the respective group.

DDI knock-down enhanced drug sensitivity of parasites. The inhibition of LmDDI1 by HIV protease inhibitors and the conservation of HIV protease-like retroviral aspartic protease fold in DDI1 proteins suggest that *Plasmodium* DDI1 could be a target of HIV protease inhibitors, which have been shown to block the development of all major stages of malaria parasites (37, 40, 42, 43, 47, 48). Hence, we assessed the PfKD parasites for susceptibility to various inhibitors and drugs, including the HIV protease inhibitors. The IC_{50} concentrations of the drugs/inhibitors tested were similar for wild type and PfKD parasites (grown in the presence of trimethoprim) (Table 1), but were less for PfKD parasites grown in the absence of trimethoprim (Table 1). The increased susceptibility to artemisinin, HIV protease inhibitors and epoxomicin was more prominent for PfKD parasites in the 2nd cycle of growth without trimethoprim, which is consistent with increased knock-down effect in the 2nd cycle. On the other hand, the IC_{50} concentrations of E64 were similar for all the parasites, indicating that increased susceptibility to artemisinin, HIV protease inhibitors and epoxomicin is specific to the knock-down effect of PfDDI1.

Table1. Susceptibility of PfDDI1 knock-down parasites to inhibitors and drugs. Wild type (WT) and PfKD parasites were assessed for susceptibility to inhibitors (cysteine protease inhibitor E64, proteasome inhibitor epoxomicin and HIV protease inhibitors) and the antimalarial artemisinin. For PfKD parasites, trimethoprim was maintained during the assay (+T), excluded during the assay (-T1) or excluded in the previous growth cycle and during the assay (-T2). ND indicates not determined.

Inhibitor	**WT**	**PfKD (+T)**	**PfKD (-T1)**	**PfKD (-T2)**
Artemisinin	19.56E-09 (3.01)	20.41E-09 (1.96)	16.99E-09 (3.52)	12.57E-09 (3.79)
E64	2.32E-06 (0.28)	2.16E-06 (0.33)	1.81E-06 (0.34)	2.09E-06 (0.04)
Lopinavir	2.23E-06 (0.38)	1.67E-06 (0.17)	1.58E-06 (0.43)	1.27E-06 (0.14)
Nelfinavir	8.92E-06 (0.38)	8.13E-06 (0.52)	7.04E-06 (0.90)	7.19E-06 (0.89)
Saquinavir	13.50E-06 (1.29)	13.54E-06 (1.23)	12.43E-06 (1.54)	10.41E-06 (2.27)
Epoxomicin	9.30E-09 (1.12)	8.19E-09 (0.67)	ND	6.75E-09 (1.11)

DDI1 associates with chromatin and DNA-protein crosslinks. ScDDI1 was first identified as one of the upregulated proteins in response to DNA damaging chemicals, and a role for ScDDI1 in DPC repair was demonstrated only recently (26). Hence, we assessed the effect of DNA damaging chemicals like hydroxyurea and methyl methanesulfonate (MMS) on the development

of PfKD parasites. The PfKD parasites showed increased susceptibility to both hydroxyurea and MMS under knock-down conditions as compared to the parasite grown under normal conditions (Figure 9A). We further investigated whether PfDDI1 is associated with chromatin. Parasites were grown with or without MMS and processed for isolation of chromatin and cytoplasmic fractions by chromatin enrichment for proteomics (ChEP). Western blot of the chromatin fraction showed the presence of H2B, a nuclear protein, and the absence of α2 proteasome subunit, a cytoplasmic protein (Figure 9B). Similarly, western blot of the cytoplasmic fraction showed the presence of α2 proteasome subunit and absence of H2B (Figure 9B), indicating purity of respective fractions. PfDDI1 was present both in the chromatin and cytoplasmic fractions, however, it had higher level in the chromatin fraction of MMS-treated parasites as compared to that of DMSO control (Figure 9B), indicating that PfDDI1 is also present in the nucleus and associates with chromatin. We next checked the effect of PfDDI knock-down on DNA-protein crosslinks (DPCs). We first optimized the procedure for preparation of etoposide-induced topoisomerase II-DPCs for HEK293T cells as has been reported earlier (Figure S6) (49). The same procedure was used to isolate DPCs from wild type *P. falciparum* 3D7 and PfKD parasites. The knock-down of PfDDI1 increased DPCs, as indicated by the increased amount of DPC-associated DNA (Figure 10A). DDI_{Myc}/cDD_{HA} was detected in DPC preparations from PfKD parasites, and had lesser level in PfKD parasites grown in the absence of trimethoprim than those grown in the presence of trimethoprim (Figure 10B), which is consistent with the knock-down level of DDI_{Myc}/cDD_{HA}. Consistently, recombinant $PfDDI1_{Myc/His}$ interacted with DPCs in a dose dependent manner, but not with purified parasite genomic DNA (Figure 10C). Hence, association of PfDDI1 with chromatin and DPCs, and accumulation of DPCs upon knock-down of PfDDI1 support a role for it in DNA damage response and repair.

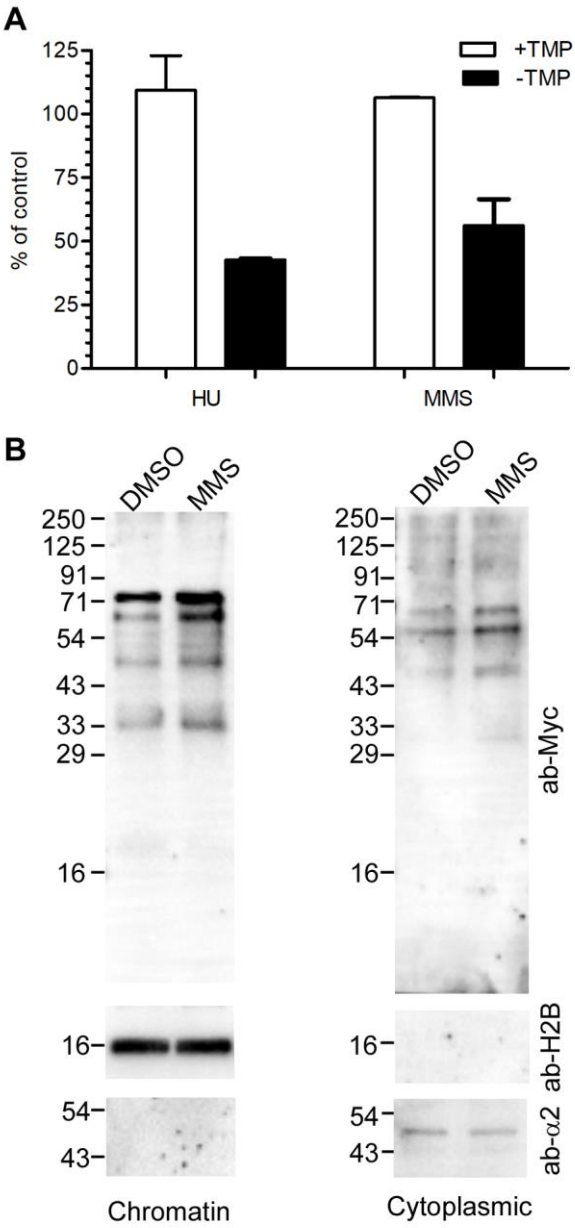

Figure 9. PfKD parasites show increased susceptibility to DNA damaging chemicals and DDI1 associates with chromatin. PfKD parasites were grown with (+TMP) or without (-TMP) trimethoprim and supplemented with hydroxyurea (HU), MMS or DMSO at mid trophozoite stage for 6 hours. The parasites were washed and grown in fresh medium (+TMP or –TMP) for 12 hours and total parasitemia was determined. The plot represents parasitemia as percent of DMSO-treated culture (% of control) for the respective group, and the data is average of two independent experiments with SD error bar. **B.** PfKD parasites were maintained in trimethoprim and treated with DMSO or MMS (0.005% v/v) at mid trophozoite stage for 6 hours. The parasites were purified and processed for separation of cytosolic and chromatin fractions as described in the methods section. The chromatin and cytoplasmic samples were evaluated for the presence of PfDDI1 by western blotting using anti-Myc antibodies (ab-Myc). Anti-histone 2B (ab-H2B) and anti-α2 proteasome subunit (ab-α2) antibodies were used to assess the purity of chromatin and cytoplasmic fractions, respectively.

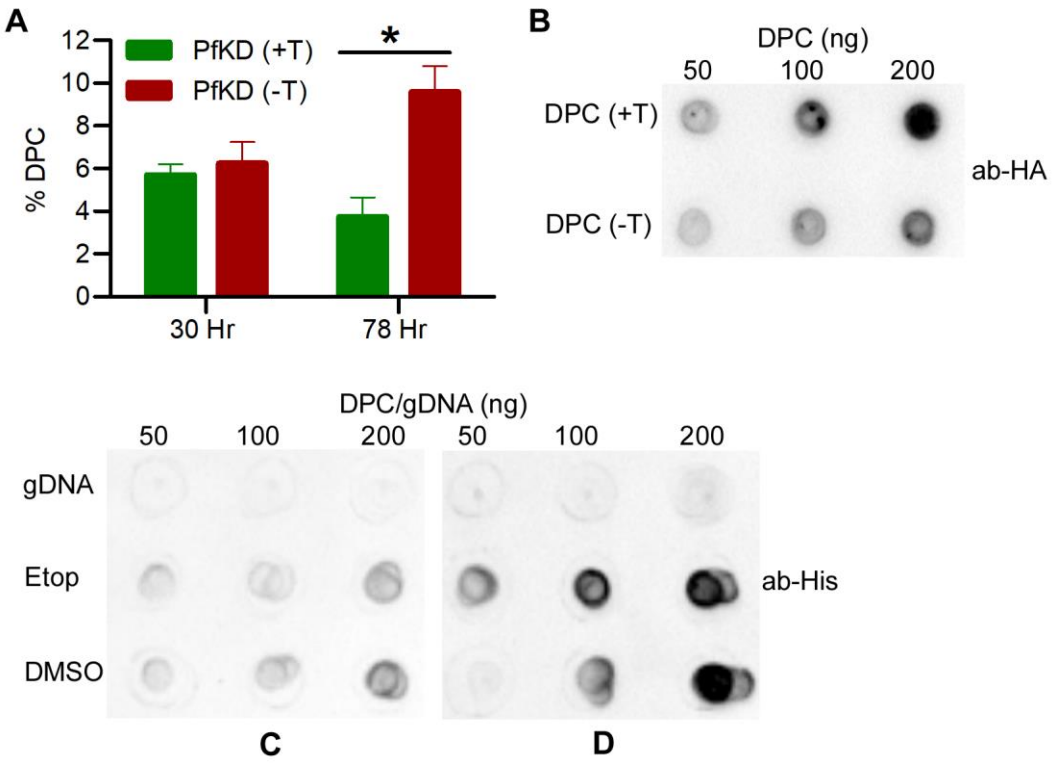

Figure 10. DPC accumulation and association with PfDDI1. DPCs were prepared from PfKD and wild type *P. falciparum* 3D7 parasites, and assessed for the associated DNA, presence of PfDDI1$_{Myc}$-cDD$_{HA}$ and interaction with recombinant PfDDI1$_{Myc/His}$. **A.** PfKD parasites were grown in the presence (+T) or absence (-T) of trimethoprim, harvested at 30 hr and 78 hr time points, and processed for isolation of DPC-associated DNA and free DNA. The graph shows DPC-associated DNA (% DPC) as percent of the total DNA present in the parasite sample. **B.** The indicated amounts of 78 hr time point DPC samples from PfKD parasites (grown in the presence (+T) or absence (-T) of trimethoprim) were spotted on a nitrocellulose membrane, and evaluated for the presence of PfDDI$_{Myc}$/cDD$_{HA}$ using anti-HA antibodies (ab-HA). **C and D.** Wild type *P. falciparum* 3D7 parasites were treated with DMSO or etoposide (Etop) and DPCs were isolated. The indicated amounts of DPCs and purified parasite gDNA (DPC/gDNA) were spotted on a nitrocellulose membrane, the membrane was overlaid with BSA (C) or recombinant PfDDI1$_{Myc/His}$ (D), and the membrane was probed using anti-His (ab-His) antibodies.

Biochemical properties of recombinant PfDDI1. To investigate biochemical properties of PfDDI1, we expressed a synthetic and codon optimized PfDDI1 coding sequence as a C-terminal Myc/His-tag (PfDDI$_{Myc/His}$) in Rosetta-gami 2(DE3)pLysS cells using the pET-26b(+) plasmid. Recombinant PfDDI$_{Myc/His}$ was purified from the soluble fraction and used for various assays. The purified protein sample contained full-length PfDDI$_{Myc/His}$ as the prominent species in addition to multiple smaller bands (Figure 11A). The full-length protein species was separated from the smaller size species by gel filtration chromatography with a relative size of 158 kDa (Figure 11B and C). The predicted size of PfDDI$_{Myc/His}$ is 46.1 kDa, suggesting that recombinant PfDDI$_{Myc/His}$

exists as an oligomer. In support of the protease activity of DDI1 proteins, LmDDI1 has been shown to hydrolyze a HIV protease peptide substrate and BSA under acidic conditions (47), the HsDDI2 has been shown to cleave Nrf1 (30), and ScDDI1 has been shown to have ubiquitin-dependent protease activity (31). However, we did not observe degradation of BSA by recombinant $PfDDI_{Myc/His}$ in our experimental settings (Figure S7A). Nonetheless, depletion of PfDDI1 caused accumulation of ubiquitinated protein (Figure S7B).

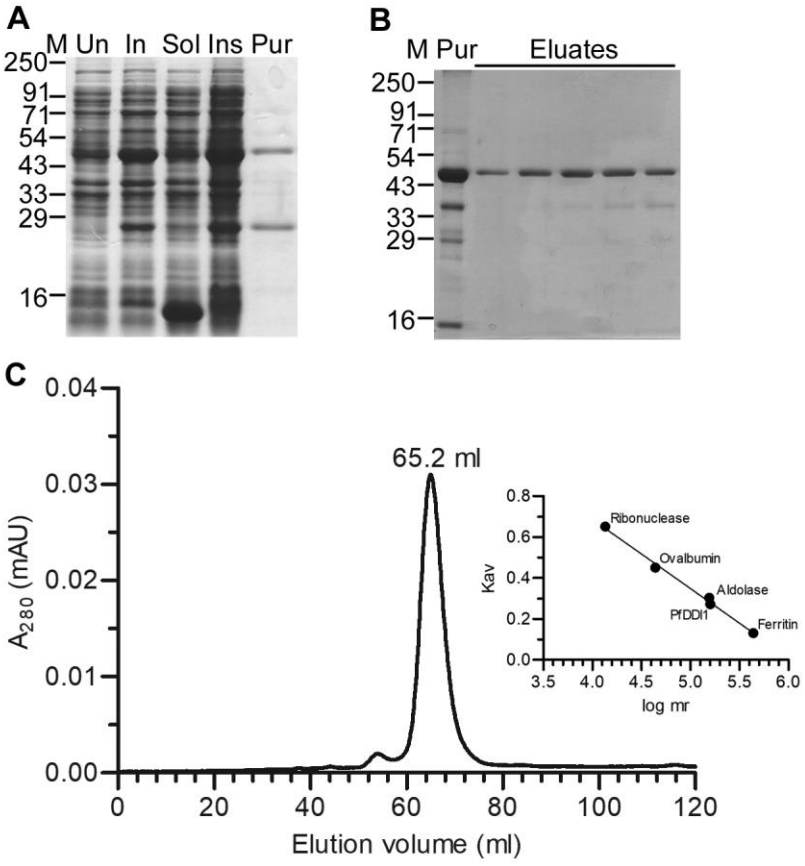

Figure 11. Production of recombinant PfDDI1. The codon optimized synthetic $PfDDI1_{Myc}$ coding region was expressed as a C-terminal His-tagged protein ($PfDDI1_{Myc/His}$) in Rosetta-gami 2(DE3) cells, purified by Ni-NTA chromatography and then by gel filtration chromatography. **A.** The coomassie stained SDS-PAGE gel shows lysates of uninduced (Un) and induced (In) cells, soluble (Sol) and insoluble (Ins) fractions of the induced cells, and Ni-NTA purified protein (Pur). **B.** The Ni-NTA purified protein (Pur) was further purified by gel filtration chromatography, and eluates were analyzed by SDS-PAGE. The coomassie stained SDS-PAGE gel shows different eluates. **C.** The first two eluates were concentrated and run on the gel filtration column and elution volume was noted. Reference protein size markers shown in the inset were also run under identical conditions, elution volumes of the reference size markers were plotted against their sizes, and used to determine the size of $PfDDI_{Myc/His}$. The sizes of protein markers are in kDa (M) in A and B.

DDI1 interacts with pre-mRNA-processing factor 19. ScDDI1 has been shown to interact with t-SNARE and v-SNARE (16, 17), ubiquitin (33, 36, 50, 51), Ho endonuclease (21), and proteasome subunits. CeDDI1/Rngo has been shown to bind ubiquitin and the 26S proteasome (28). SpDDI1/Mud1 binds K48-linked polyubiquitin (24). Hence, we immunoprecipitated $PfDDI_{Myc}$/cDD_{HA} and subjected it to mass spectrometry to identify the interacting proteins. 62 proteins were reproducibly present in the immunoprecipitate from three biological repeats (Table S2), including the *P. falciparum* pre-mRNA-processing factor 19 (PfPRP19), proteins predicted to associated with the ubiquitin proteasome system and protein translation. Since the human PSO4/PRP19 is an E3 ubiquitin ligase and has been shown to play critical roles in multiple DNA repair pathways and mRNA splicing (52, 53), we produced recombinant PfPRP19 and assessed it for interaction with recombinant $PfDDI1_{Myc/His}$ by protein-protein overlay assay. Both the recombinant proteins showed dose-dependent interaction (Figure 12, Figure S8), indicating that these two proteins interact directly. We speculate that PfPRP19 may mediate the chromatin association of PfDDI1, as PSO4/PRP19 proteins, but not PfDDI1, contain DNA-binding domains.

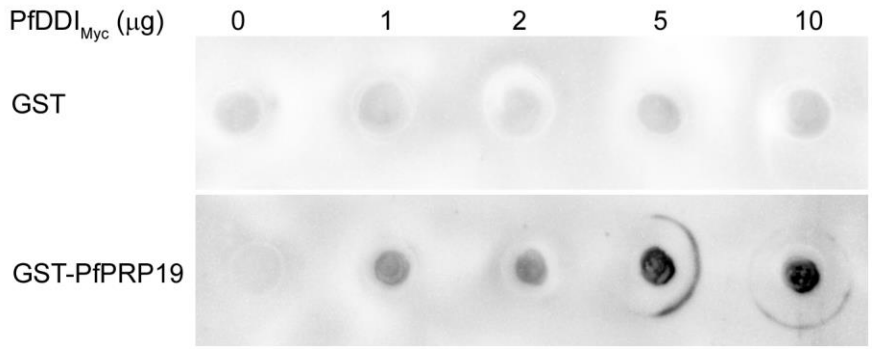

Figure 12. PfDDI1-PfPRP19 overlay assay. The blot containing spots of the indicated amounts of recombinant $PfDDI_{Myc/His}$ ($PfDDI_{Myc}$) was overlaid with recombinant GST or GST/PfPRP19 and probed with anti-GST antibodies.

PfDDI1 reversed the hypersecretion phenotype of ScDDI1 knock-out strain. We generated *S. cerevisiae* strains lacking the DDI1 gene (ScDDIko). The ScDDIko strain was complemented by expressing wild type PfDDI1 (Sc-wPfDDIki) or catalytic mutant of PfDDI1 (Sc-mPfDDIki) under the native ScDDI1 promoter (Figure S9). These strains were compared with the wild type strain for growth under various conditions. We did not observe any growth defect in ScDDIko, Sc-wPfDDIki and Sc-mPfDDIki strains as compared to the wild type strain (Figure S9). The ScDDIko

strain showed hypersecretion phenotype as compared to the wild type, which was reversed to wild type level in Sc-wPfDDIki strain (Figure S9), indicating that PfDDI1 is functionally similar to ScDDI1 as a negative regulator of protein secretion. ScDDIko, Sc-wPfDDIki and Sc-mPfDDIki strains were as sensitive as the wild type strain to agents causing DNA damage (hydroxyurea), DNA-protein crosslinks (etoposide), antimalarials (artemisinin and chloroquine) and HIV protease inhibitors (lopinavir and nelfinavir) (data not shown).

DISCUSSION

DDI1 proteins have been shown to have important roles in several cellular processes, including negative regulation of protein secretion, repair of DPCs and ubiquitin-dependent proteolysis. Several of these functions are associated with the presence of UBL, RVP and UBA domains in DDI1 proteins, including the interaction with ubiquitin chains via the UBA and UBL domains, interaction with the proteasome via UBL domain and cleavage of selected substrates via the RVP domain. LmDDI1 has also been proposed to be the major target of HIV protease inhibitors, which have also been shown to block the development of malaria parasites at multiple stages. However, the *Plasmodium* DDI1 has not been studied yet. We report functional characterization of *Plasmodium* DDI1 using the rodent malaria parasite *P. berghei* and the human malaria parasite *P. falciparum*, which revealed that it is indispensable for parasite development, is a potential target of HIV protease inhibitors and contributes to DPC repair.

PfDDI1 contains the UBL and RVP domains, but lacks the UBA domain. DDI1 homologs are present in all apicomplexa parasites, which vary in size and domain organization. Of the 54 Apicomplexan DDI1 proteins available in the EuPathDB, all contain UBL and RVP domains, and 10 DDI1 proteins also contain the UBA domain. Interestingly, the DDI1 proteins of *B. divergens* and *B. bigemina* contain a putative DUF676 domain in addition to the UBL and RVP domains. Except the Babesiidae parasites, domain organization is conserved among parasites of the same family. Although Apicomplexan DDI1 proteins vary in size from 275 amino acid residues (*G. niphandrodes*) to 1191 amino acid residues (*B. bigemina*), the differences in domain architecture is unlikely due to the differences in protein size. For example, *C. hominis* DDI1 is 384 amino acids long and contains all three domains, whereas *B. bigemina* DDI1 is 1191 amino acids long but contains UBL and RVP domains only. The DUF676 domain is predicted to be a serine esterase and is unique to *B. divergens* and *B. bigemina*, as none of the DDI1 proteins available in the UniProtKB database contains the DUF676 domain. It is a characteristic of the alpha/beta hydrolase superfamily, which contains diverse enzymes (esterases, lipases, proteases, epoxide hydrolases, peroxidases and dehalogenases). The closest related proteins to DUF676 domain of Babesia DDI1 are FAM135A proteins. However, there is no report of the characterization of any FAM135A protein. Interestingly, a search of the Apicomplexa genomes using the sequence of DUF676-containing region of *B. bigemina* DDI1 identified DUF676-containing proteins in all parasites

except *Plasmodium* and *Piliocolobus*. This suggests that DDI1 and the DUF676-containing protein function together in some pathway. It may be an oversight to predict a role for the DUF676 domain or any additional property it might impart to the DDI1 proteins of *B. divergens* and *B. bigemina*. Nonetheless, this domain may confer ubiquitin esterase activity to DDI1 for cleavage of non-lysine ubiquitin chains. Ubiquitin esterase activity is important to cleave the ubiquitin linked to Ser, Cys or Thr residue of the substrate (54, 55). A comparative analysis of the domain organization of DDI1 proteins indicates conservation of UBL and RVP domains in Apicomplexan DDI1 proteins. The diversity in domain architecture might impart species-specific functions to DDI1 proteins, which could enable these parasites to develop in diverse host environments.

Expression of *Plasmodium* DDI1 in asexual erythrocytic, gametocyte, sporozoite and liver stages is in agreement with stage-wise transcription and proteomics data for *Plasmodium* DDI1 proteins, and indicate a major role for it throughout the parasite development. Failure to knock-out the DDI1 gene and drastic growth defects in DDI1 knock-down parasites support an essential role of *Plasmodium* DDI1 during asexual erythrocytic stage development, which is likely be critical for non-erythrocytic stage development also. The knock-down effect of DDI1 was stronger in *P. berghei* than that in *P. falciparum*, which could be due to host immune response in the first case. Intrinsic stability of PfDDI1 and degradation efficiency of *Plasmodium* UPS may contribute to the partial knock-down effect in *P. falciparum*. *T. gondii* and *L. major* DDI1 proteins have also been shown to be critical for parasite development (37, 39), which is consistent with our data and support a key role for DDI1 in apicomplexan parasites.

DDI1 knock-down in *P. berghei* not only decreased virulence with self-resolving infection, it also elicited protective immunity to subsequent lethal infections of wild type *P. berghei* ANKA and *P. yoelii* 17XNL. On the other hand, immunization of mice with recombinant PbDDI1 did not induce any protection, suggesting that protective immunity could be due to the presence of anti-parasite antibodies and cellular immune responses against the whole parasite. As in our study, prior infection of mice with knock-out parasites (purine nucleoside phosphorylase, plasmepsin 4, plasmepsin-4 + merozoite surface protein-7, nucleoside transporter 1) has also been shown to cause self-limiting infection with development of protective immunity (56-59). Attenuated parasites are candidates in efforts to develop a whole organism malaria vaccine and PfDDI1 knock-down parasites could add to the arsenal of whole organism blood stage malaria vaccine candidates.

Knock-down of PfDDI1 increased parasite sensitivity to artemisinin, epoxomicin and HIV protease inhibitors, which suggested PfDDI1 as a target or role for it in the associated pathways. The increased susceptibility to epoxomicin suggests a role of PfDDI in proteasome function, which is also consistent with the accumulation of ubiquitinated proteins upon PfDDI1 knock-down. Human DDI2 has been shown to be required for proteasome biogenesis (29, 30), DDI1 proteins of human, *S. cerevisiae* and *T. gondii* have been shown to cleave high molecular weight ubiquitin conjugates (32, 39), which support a role of DDI1 proteins in modulating proteasome function. Hence, depletion of PfDDI1 might have rendered the proteasome less efficient, thereby, causing increased susceptibility to epoxomicin. Artemisinin has been reported to compromise the proteasome function (60), suggesting that increased susceptibility of PfDDI1 knock-down parasites to artemisinin could be due to the compromised proteasome system. Increased susceptibility to HIV protease inhibitors upon knock-down of PfDDI1 suggests that it is a target of these inhibitors. Our result is consistent with the previous studies indicating that *L. major* DDI1 is the major target of the anti-leishmanial activity of HIV protease inhibitors (37, 47). However, it is possible that HIV protease inhibitors also inhibit other targets in malaria parasites, as has been reported for Plasmepsin-V in malaria parasites and multiple pathways in mammalian cells, including inhibition of the chymotryptic activity of proteasome, induction of endoplasmic reticulum stress and cell cycle arrest (61-66). .

PfDDI1 knock-down parasites showed increased susceptibility to DNA damaging chemicals and accumulation of DPCs. This was further corroborated by the association of PfDDI1 with chromatin and DPCs, which indicates a role for PfDDI1 in DNA damage response and DPC repair. A role for ScDDI1 in DPC repair has been recently proposed (26), which is in agreement with our data supporting involvement of PfDDI1 in DPC repair. Although the mechanism by which DDI1 contributes to the repair of DPCs is not known, DDI1 could help in degradation of DPCs directly owing to its ubiquitin-dependent protease activity and/or by recruiting the repair pathway proteins (31).

In contrast to the previously reported protease activity of LmDDI1 (47), we did not observe degradation of BSA by recombinant PfDDI1 under our experimental settings. Nonetheless, depletion of PfDDI1 caused accumulation of ubiquitinated proteins, which may be a result of the

reduced PfDDI1 activity or compromised proteasome function. Ubiquitin-dependent protease activity has been demonstrated for some DDI1 proteins (31, 32), and PfDDI1 may be a ubiquitin-dependent protease. PfDDI1 interacted with putative PfPRP19, a homolog of human and *S. cerevisiae* PSO4/PRP19, which is an E3 ubiquitin ligase and has been found to have critical roles in mRNA splicing and multiple DNA repair pathways (52, 53). PfDDI1-PfPRP19 interaction in our study is in line with the involvement of the homologs of these two proteins in DNA damage repair. We speculate that chromatin association of PfDDI1 may be mediated by PfPRP19, as PfPRP19 and other PSO4/PRP19 proteins, but not PfDDI1, contain a DNA-binding domain and a nuclear localization signal.

Expression of PfDDDI1 in ScDDI1 knock-out strain reversed the hypersecretion phenotype that has been reported previously (16), suggesting that PfDDI1 has a role in regulation of protein secretion. Notably, humans treated with HIV protease inhibitor-based antiretroviral therapy showed reduced incidences of malaria compared to the group treated with non-protease inhibitor-based anti-retroviral therapy (45). It is possible that HIV protease inhibitor-treated parasites and DDI1 knock-down *P. berghei* parasites secrete more proteins in the host than wild type parasites, which would act as antigens and elicit stronger immune response than the wild type parasites. ScDDIko, Sc-wPfDDIki and Sc-mPfDDIki strains were similarly sensitive to agents causing DNA damage and DPC, suggesting that deletion of ScDDI1 alone does not alter sensitivity to these agents. Previous studies related to the role of ScDDI1 in DNA damage and DPC repair pathways have been done in combination with additional genes and knock-out of ScDDI1 alone did not affect sensitivity to some of these chemicals (26, 27).

During the preparation of this manuscript, we also noted two independent studies on *Plasmodium* DDI1 in bioRxiv, and one of the studies, in agreement with our results, demonstrates the essentiality of PfDDI1 for asexual stage parasite development (67, 68).

We demonstrate that DDI1 is essential for the malaria parasite development, DDI1 knock-down parasites confer protective immunity and it could be a target of HIV protease inhibitors, which make it a dual-target candidate for developing antimalarial therapeutic agents. Accumulation of DPCs upon DDI1 knock-down and association of PfDDI1 with chromatin and DPCs support a role for it in DNA damage response and DPC repair. The functional significance of the association of PfDDI1 with chromatin and DPCs needs to be investigated.

MATERIALS AND METHODS

All the biochemicals were from Merck, Sigma-Aldrich or SERVA unless otherwise mentioned. Cell culture reagents were from Gibco and Lonza. DNA modifying enzymes were from New England Biolabs, Thermo Fisher Scientific or TaKaRa. DNA and RNA isolation kits were from Qiagen or MACHEREY-NAGEL. Ni-NTA agarose was from Qiagen or Thermo Fisher Scientific. SuperSignal West Chemiluminescent Substrates were from Pierce. Secondary antibodies were from Pierce or Sigma-Aldrich. ProLong^{TM} gold anti-fade reagent was from Thermo Fischer Scientific. *P. falciparum* and *P. berghei* ANKA strains were obtained from the Malaria Research and Reagent Reference Resource centre (MR4). Basic Parasite Nucleofector^{TM} Kit 2 was from Lonza. Inhibitors and drugs (etoposide, trimethoprim, hydroxyurea, methyl methanesulfonate MMS, HIV protease inhibitors, E64, chloroquine and artemisinin) were from Sigma-Aldrich, Santa Cruz Biotechnology, Biorbyt, Selleckchem or Tocris Bioscience. Human blood was collected from healthy volunteers after taking written consent under medical supervision at the medical dispensary of the institute according to the protocols approved by Institutional Ethics Committee (IEC) of Centre from Cellular and Molecular Biology, Hyderabad, India. Animals used in this study were maintained at standard environmental conditions (22–25°C, 40–70% humidity, and 12:12 hour dark/light photoperiod), and all animal experiments were carried out according to the protocols approved by the Institutional Animal Ethics Committees (IAEC) of Centre from Cellular and Molecular Biology, Hyderabad, India.

Sequence analysis of DDI1 proteins. The PfDDI1 amino acid sequence (PF14_0090) was obtained from the *Plasmodium* genome database PlasmoDB by BLAST search using ScDDI1 amino acid sequence (P40087) as a query. The sequences of DDI1 homologs were obtained from the UniProtKB and EuPathDB databases using PfDDI1 and ScDDI1 amino acid sequences as queries. Sequence alignment of DDI1 proteins was performed using the Clustal Omega (https://www.ebi.ac.uk/Tools/msa/clustalo/). Sequences of DDI1 proteins were analyzed for the presence of conserved domains and catalytic site using the Conserved Domain Database (https://www.ncbi.nlm.nih.gov/Structure/cdd/wrpsb.cgi) and Pfam (http://pfam.xfam.org/) softwares. For phylogenetic analysis, sequences were aligned using MUSCLE, alignment was curated with Gblocks, phylogenetic tree was constructed using PhyML and edited with TreeDyn (http://www.phylogeny.fr/simple_phylogeny.cgi). A structure of full-length DDI1 is not available,

yet. Hence, we superimposed the AlphaFold structure of PfDDI1 on the reported structures of ScDDI1 UBL (PDB IDs: 2N7E) and RVP (PDB ID: 2I1A) domains using the PyMOL Molecular Graphics System. The DDI1 proteins of representative Apicomplexan parasites were also analyzed for the presence of UBL, RVP and UBA domains by the Swiss Model online software. Homology models of *Cytauxzoon felis* UBA (Cf-UBA), *Theilaria annulata* UBA (Ta-UBA) and *Gregarina niphandrodes* UBL (Gn-UBL) were generated using the closest related templates structures (PDB: 1Z96 for *S. pombe* UBA (39.47% sequence identity with Cf-UBA and 26.32% Ta-UBA), 2N7E for ScDDI1 UBL (15.94% sequence identity with Gn-UBL)) by Swiss Model online software. The modelled structures were superimposed on the template structures and RMSD values were calculated using the PyMOL Molecular Graphics System, version 1.3, Schrodinger, LLC.

Parasite culture. *P. falciparum* 3D7 and D10 strains were cultured in RPMI-1640 medium (supplemented with 2.0 g/l glucose, 0.5% AlbuMAX II, 41.1 mg/l hypoxanthine, 300 mg/l glutamine, 25 mg/l gentamicin and RBCs at 2% hematocrit) at 37°C under a gas mixture (5% CO_2 + 5% O_2 + 90% N_2). Giemsa stained smears of the culture were regularly prepared and observed under the 100× magnification of a light microscope to monitor parasite development. Synchrony was maintained by treating the cultures at ring stage with 5% sorbitol (69). The cultures were harvested at 10-15% parasitemia whenever required and parasites were purified from infected-RBCs by saponin (0.1% in PBS) lysis method. For *P. berghei* ANKA, a frozen stock was injected intra-peritoneally into a 4-6 weeks old naïve female BALB/c mice. The infection and was monitored by observing Giemsa stained smears of the tail-snip blood on every other day of post-infection. Mice were sacrificed at 6-10% parasitemia, the blood was collected by cardiac puncture in Alsever's solution (2.05 % Glucose, 0.8% sodium citrate, 0.055% citric acid, and 0.42% sodium chloride) and the cell pellet was treated with 0.1% saponin to isolate parasites. The pellets of purified parasites were used immediately or stored at -80°C till further use. *P. falciparum* gametocytes were obtained by inducing gametocytogenesis with spent medium as has been described previously (70, 71). Gametocyte development was monitored by observing Giemsa stained smears of the culture on daily basis and samples at different gametocyte stages were collected to determine localization of PfDDI1. Genomic DNA was isolated from trophozoite/schizont stage parasites using the Puregene Blood Core Kit B as instructed by the manufacturer.

Production of recombinant proteins. The complete PfDDI1 coding region was amplified from *P. falciparum* genomic DNA using primers PfDdi-expF/PfDdi-expR, cloned into the pQE-30 plasmid at BamHI-HindIII to obtain pQE30-PfDDI1, and transformed into M15(pREP4) *E. coli* cells. pQE30-PfDDI1 would express PfDDI1 as an N-terminal His-tagged protein, facilitating purification of the protein by Ni-NTA affinity chromatography. For purification of $_{His}$PfDDI1, the IPTG-induced cell pellet was resuspended in urea buffer (8 M Urea, 10 mM Tris, 250 mM NaCl, pH 8.0), incubated for 30 minutes at room temperature, and the lysate was sonicated for 5 minutes (9 seconds on-off cycle at 20% amplitude) using SONICS vibra-cell sonicator. The lysate was centrifuged at 18000g for 30 minutes at 4^{o}C, the supernatant was supplemented with imidazole (10 mM) and incubated with Ni-NTA resin (0.2 ml resin/5g of initial cell pellet) at room temperature for 30 minutes. The resin was transferred to a column and washed with urea buffer containing imidazole (20-50 mM). The bound protein was eluted with elution buffer (250 mM imidazole in urea buffer) and resolved in a 12% SDS-PAGE. Elution fractions enriched with His-PfDDI1 were pooled and dialyzed against the refolding buffer-1 (10 mM Tris, 1 mM GSH, 0.5 mM GSSG, 50 mM NaCl, 10% glycerol, pH 8.0) for 12 hours at 4^{o}C, followed by against the refolding buffer-2 (10 mM Tris, 50 mM NaCl, 0.5 mM DTT, pH-8.0) with 2 changes at an interval of 3 hours. The refolded protein was concentrated using a 3-kDa cut off Amicon Ultra-15, estimated by Bradford assay, and stored at -80°C till further use.

A codon optimized synthetic version of PfDDI1 gene with C-terminal Myc-tag (synPfDDI1$_{Myc}$) was purchased from Life Technologies (pMA-DDI), and used as a template for amplification of PfDDI1$_{Myc}$ coding region using PRPsyn-Fchis/PRPsyn-Rchis primers. The PCR fragment was cloned into pET26B at NdeI-XhoI site to obtain pET26B-PfDDI1$_{Myc}$ plasmid, and transformed into the Rosetta-gami 2(DE3) *E. coli* cells for expression. The recombinant protein would be expressed with a C-terminal His-tag (PfDDI1$_{Myc/His}$), enabling purification by Ni-NTA chromatography. A pET26B-PfDDI1$_{Myc}$ expression clone was grown in LB broth and induced with IPTG (0.5 mM final) at an OD_{600} of 0.6 at 20^{o}C for 4 hours with shaking at 225 rpm. The induced cell pellet was resuspended in lysis buffer (20 mM Tris, 500 mM NaCl, 20 mM Imidazole, 2 mM β-mercaptoethanol, pH 8; lysozyme at 1 mg/ml; 5 ml buffer/g pellet), incubated for 30 min at 4°C and sonicated (30% amp with 5 sec on/off for 30 min) using SONICS vibra -ell Ultrasonic. The lysate was centrifuged at 39191g for 1 hour at 4°C, the supernatant was applied on the HisTrap HP column (GE healthcare), washed with lysis buffer, and the bound proteins were eluted (20 mM

Tris, 500 mM NaCl, 0-250 mM Imidazole, 2 mM β-mercaptoethanol, pH 8). The elution fractions were resolved in 12% SDS-PAGE and the fractions with high purity of the recombinant protein were concentrated using a 50 kDa cutoff Amicon Ultra concentrator. The concentrated protein was further purified by gel filtration chromatography (Hiload superde x 200 16/600, GE healthcare) with buffer (20 mM Tris, 150 mM NaCl, 2 mM β-mercaptoethanol, pH 7.5). The elution fractions were resolved on 12% SDS-PAGE to check for purity, fractions containing the pure protein were pooled, concentrated using a 10 kDa cut off Amicon Ultra-15, quantified using the BCA method (Thermo Fisher Scientific), and used immediately or stored at -80°C till further use. To determine the size of PfDDI1$_{Myc/His}$, reference protein size markers and gel filtration purified PfDDI$_{Myc/His}$ were loaded on the column (Hiload superdex 200 16/600, GE healthcare) with buffer (20 mM Tris, 150 mM NaCl, 2 mM β-mercaptoethanol, pH 7.5). The elution volumes of reference protein size markers were plotted against their sizes, and the plot was used to determine the size of PfDDI$_{Myc/His}$.

Wild type *P. berghei* DDI1 (PbDDI1) was amplified from *P. berghei* gDNA using PbDdiexpF/PbDdiexpRm primers (PbDdiexpRm encodes for an in-frame Myc-tag). The PCR fragment was cloned into pRSET-A at HindIII-XhoI site to obtain pRSETA-wPbDDI1$_{Myc}$ expression plasmid. A catalytic mutant of PbDDI1 (D268A) was generated by overlap PCR. Briefly, the 5'- and 3'-fragments of PbDDI1 coding region were amplified from the pRSETA-wtPbPRPmyc plasmid using PbDdiexpF/Pbddimut-R and PbDdimut-F/PbDdiexpRm primer sets, respectively. The two fragments overlapped around the mutation site, facilitating recombination by PCR using PbDdiexpF/PbDdiexpRm primers. The recombined fragment was cloned into pRSET-A at BamHI-HindIII sites to obtain pRSETA-mPbDDI1$_{Myc}$ expression plasmid. The expression plasmids were transformed into BL21-CodonPlus (DE3) *E. coli* cells, which would express recombinant proteins with N-terminal His-tag, thereby enabling purification of by Ni-NTA affinity chromatography. The wild type (wPbDDI$_{Myc}$) and mutant (mPbDDI$_{Myc}$) recombinant proteins were purified from the IPTG-induced cells of respective expression clones under native conditions. Briefly, the expression clones were grown in LB broth and expression was induced with IPTG (1 mM final) at an OD_{600} of 0.6 at 20ºC for 4 hours with shaking at 225 rpm. The cell pellet was resuspended in native buffer (50 mM NaH_2PO_4, 100 mM NaCl, pH 8.0; lysozyme at 1 mg/ml; 5 ml buffer/g pellet), incubated in ice for 30 min and sonicated for 4 min (9 second pulses at 20% amplitude) using SONICS Vibra Cell Ultrasonic Processor. The lysate was centrifuged at

25,000g for 30 min, the supernatant was supplemented with imidazole (10 mM) and incubated with Ni-NTA agarose resin (0.4 ml slurry/g weight of the initial cell pellet) for 30-45 min at 4°C. The resin suspension was transferred to a column, washed with wash buffer (native buffer with 20-50 mM imidazole) and the bound proteins were eluted with elution buffer (native buffer with 250 mM imidazole). The elution fractions were resolved on 12% SDS-PAGE. The fractions enriched with the recombinant protein were pooled and dialyzed against the storage buffer (20 mM Tris-Cl, 50 mM NaCl, pH 8.0) using a 10 kDa cut off dialysis tubing at 4°C. The dialyzed protein was concentrated using a 10 kDa cut off Amicon Ultra-15, quantified using the BCA method (Thermo Fisher Scientific), and stored at -80°C.

Protease assay. The assay samples containing 2 µg BSA and 1 µg recombinant $PfDDI_{Myc/His}$ in 30 µl buffer (20 mM Tris, 50 mM NaCl, 2 mM β-mercaptoethanol, pH 7.0 or 7.5) were incubated at 37°C. The reaction was stopped by adding 6 µl of 4 × SDS-PAGE sample buffer (1 × buffer contains 50 mM Tris-HCl, 20% glycerol, 2% SDS, 1% β-mercaptoethanol, 0.01% bromophenol blue, pH 6.8) to assay samples at different time points (0, 1, 2.5, 5 and 10 hours). Control assay samples contained the same amount of BSA or recombinant $PfDDI_{Myc/His}$, which were incubated at 37°C for 10 hours and stopped by adding 6 µl of 4 × SDS-PAGE sample buffer to the sample. The reaction and control samples were resolved in 12% SDS-PAGE and stained with coomassie brilliant blue.

Generation of anti-PfDDI antiserum. Three months old two female Wistar rats were immunized intraperitoneally with emulsion of recombinant $_{His}$PfDDI1 (200 µg/immunization) in Freund's complete (day 0) or incomplete adjuvant (day 21, 42, 84 and 105). Blood was collected (day -1, 14, 35, 70, 91 and 125). The day-125 antiserum was adsorbed with *E. coli* proteins to eliminate the antibodies cross-reactive with bacterial proteins as has been described earlier (72). The adsorbed PfDDI1antiserum was supplemented with 0.01% sodium azide and glycerol (50% final) for storage at -80^{o}C, and used to determine expression and localization of PfDDI1 or PbDDI1 in various parasite stages.

Western blotting and immunofluorescence assay. A synchronized culture of *P. falciparum* 3D7 (~10% parasitemia) was harvested at ring, early trophozoite, mid-trophozoite and late trophozoite/schizont stages. Parasites were purified by saponin lysis, resuspended in 4x pellet volume of SDS-PAGE sample buffer, equal amounts of lysates (corresponding to approximately

1×10^8 parasites/lane) were resolved on 12% SDS-PAGE and the proteins were transferred onto the PVDF membrane. The membrane was sequentially incubated at room temperature with blocking buffer (5% non-fat milk in TBS-T) for 1 hour, rat PfDDI1 antiserum (at 1/4000 dilution in blocking buffer) for 1 hour, blocking buffer for washing, and HRP-conjugated goat anti-rat IgG (at 1/10,000 dilution in blocking buffer). The membrane was washed with blocking buffer followed by with PBS, incubated with the Supersignal™ west chemiluminescent substrate, and the signal was taken on X-ray film. PbDDI1 expression in *P. berghei* erythrocytic stage parasites was checked by western blotting using rat PfDDI1 antiserum as has been described of *P. falciparum*.

For localization of PfDDI1, different developmental stages of *P. falciparum* erythrocytic and gametocyte cultures were collected, the cells were washed with PBS, immobilized on poly-L coated slides, fixed (4% paraformaldehyde/0.002% glutaraldehyde in PBS) for 45 minutes, and permeabilized (0.01% Triton-X 100). The slides were sequentially incubated at room temperature in blocking buffer (3% BSA in PBS), rat PfDDI1 antiserum (at 1/500 dilution in blocking buffer), and Alexa flour-488 conjugated donkey anti-rat IgG or Alexa fluor-594 conjugated donkey anti-rat IgG (at 1/2000 dilution in blocking buffer, with DAPI at 10 µg/ml). The slides were air dried, mounted with ProLong Gold antifade, and images were captured using Zeiss AxioImager Z with Apotome or Zeiss Axioimager 2 microscope under the 100× objective. Images were processed using Zeiss Axiovision and Adobe Photoshop softwares. For PbDDI1 localization in *P. berghei* erythrocytic trophozoites, 10 µl blood was collected from the tail-snip of a *P. berghei* ANKA-infected mouse and the cells were processed for IFA using rat PfDDI1 antiserum as has been described for PfDDI1 localization in *P. falciparum*. For PbDDI localization in sporozoite and liver stages, female Anopheles mosquitos were fed on *P. berghei* ANKA-infected BALB/c mice and dissected on day 18 for isolation of salivary gland sporozoites. The sporozoites were spotted on a glass slide and air dried. 1×10^4 sporozoites were added on the HepG2 monolayer cultured in DMEM with 10% FBS in labtek chamber slides and grown for 36 hours. The sporozoite and liver stage samples were processed for IFA using rat PfDDI1 antiserum for PbDDI1, mouse anti-circumsporozoite protein (CSP) antibodies for the sporozoites, and rabbit anti-upregulated in infective sporozoites-4 (UIS-4) antibodies for the liver stage as has been described earlier (73). The slides were incubated with appropriate secondary antibodies (Alexa Fluor-594 conjugated donkey anti-rat IgG, Alexa flour-488 conjugated rabbit anti-mouse IgG for CSP and Alexa flour-

488 conjugated mouse anti-rabbit IgG for UIS-8), observed under the 40× objective, images were captured and processed as has been described for PfDDI1 localization in *P. falciparum*.

Construction of transfection plasmids. The PbDDI1 gene was targeted for knock-out and knock-down using double cross-over homologous recombination approach. The 5'-UTR (flank 1) and 3'-UTR (flank 2) of PbDDI1 were amplified from *P. berghei* genomic DNA using PbDdi1-Fl1F/ PbDdi1-Fl1R and PbDdi1-Fl2F/PbDdi1-Fl2R primer sets, respectively. The flank 1 and flank 2 were cloned into the HB-DJ1KO plasmid at NotI-KpnI and AvrII-KasI sites, respectively, to obtain HB-PbDDI-(FL1+FL2) plasmid. The GFP coding sequence was excised from pGT-GFPbsc with KpnI-XhoI and subcloned into the similarly digested HB-PbDDI-(FL1+FL2) to obtain HB-pbDDIKO plasmid. For construction of knock-down plasmid, the $PfDDI_{Myc}$ coding sequence was amplified from the *P. falciparum* genomic DNA using DDiexp-F/DDimyc Rep-R primers, digested with KpnI-XhoI and subcloned into the similarly digested HB-PbDDIKO plasmid in place of GFP to obtain HB-PfDDIKI plasmid. The *E. coli* mutant DHFR coding sequence with HA-tag (cDD_{HA}) was amplified from the pPM2GDBvm plasmid (a kind gift from Dr. Praveen Balabaskaran Nina) using cDD-F/cDD-R primers, and cloned into the pGT-GFPbsc plasmid at KpnI/XhoI sites to obtain pGT-cDD_{HA} plasmid. The $PfDDI_{Myc}$ coding sequence was amplified from HB-PfDDIKI plasmid using the PfDdi-reF/PfDdi-cDDR primers and cloned into the pGT-cDD_{HA} plasmid at BglII-BamHI site to obtain the pGT-PfDDI-cDD_{HA} plasmid. The pGT-$PfDDI_{Myc}$/cDD_{HA} plasmid was digested with BglII-XhoI to release the $PfDDI_{Myc}$/cDD_{HA} insert, which was cloned into the similarly digested HB-DDKI plasmid to obtain HB-pbDDIKD vector. All the flanks and coding regions were sequenced to ensure that they were free of undesired mutations, and the presence of different regions was confirmed by digestion with region-specific restriction enzymes. The HB-pbDDIKO and HB-pbDDIKD plasmids were purified using the NucleoBond® Xtra Midi plasmid DNA purification kit (MACHEREY-NAGEL), linearized with NotI-KasI, gel purified to obtain pbDDIKO and pbDDIKD transfection constructs, and used for transfection of *P. berghei*.

The flank 1 of HB-pbDDIKD was excised with NotI-BglII, the ends of plasmid backbone were filled and ligated. The flank 2 of this plasmid was excised with AvrII-KasI, and the plasmid backbone was ligated with the similarly digested PfDDI1-3'UTR, which was amplified from *P. falciparum* genomic DNA using PfDDi3'U-F/PfDDi3'U-R primers. The final plasmid was called

HF-pfDDIKD, which contains PfDDI1$_{Myc}$/cDD$_{HA}$ coding region as fank1 and PfDDI1-3'UTR as flank2. HF-pfDDIKD was digested with region-specific restriction enzymes to ensure the presence of different regions, purified using the NucleoBond® Midi plasmid DNA purification kit (MACHEREY-NAGEL), and used for transfection of *P. falciparum*.

Generation of PbKD parasites. A frozen stock of *P. berghei* ANKA was injected intraperitoneally into a naïve BALB/c mouse. Infection was monitored and blood was collected as has been described in the parasite culture section. The cells were washed with FBS-RPMI medium (RPMI1640, 20% FBS, 2 g/l Glucose, 2 g/l, Sodium bicarbonate, 41.1 mg/ml Hypoxanthine, pH-7.5), resuspended in FBS-RPMI medium at 2% hematocrit, gassed (5% CO_2, 5% O_2, 90% N_2), and incubated at 37^{o}C for 12-14 hours with shaking of 55 rpm. Parasites were purified on a 65% Nycodenz gradient cushion when the majority of the parasites reached schizont stage. The cells were washed with FBS-RPMI medium and aliquoted, each with 15-20 µl of packed cell volume. An aliquot was mixed with 100 µl of Amaxa T cell nucleofactor and 2.5-5 µg of pbDDIKO or pbDDIKD transfection constructs, pulsed using the Amaxa Nucleofector (U303 program), and injected intravenously into a naive mouse. One day after the transfection, the infected mouse was given drinking water with 70 µg/ml pyrimethamine (for knock-out) or 70 µg/ml pyrimethamine + 40 µg/ml trimethoprim (for knock-down) for 7-10 days to selected resistant parasites. Blood Smears were checked for the presence of parasites on day 7 post-transfection and then every other day. The genomic DNA and lysates of resistant parasites were checked for integration and expression of desired protein by PCR and western blotting, respectively. Cloned lines of *P. berghei* knock-down parasites (PbKD) were obtained infecting 15 naïve BALB/c mice intravenously with 200 µl of diluted parasite suspension (0.5 parasite/mouse). Mice were given pyrimethamine + trimethoprim in drinking water and infection was monitored by making blood smears. Blood was collected from infected mice as has been described in the parasite culture section. Part of the blood was used for making frozen stocks for later use, and the remaining blood was processed for isolation of genomic DNA and preparation of parasite lysate to check for desired integration and expression of the desired protein by PCR and western blotting, respectively.

The genomic DNAs of wild type parasites and two PbKD clonal lines were assessed for the presence of recombinant locus by PCR with primers specific for 5' specific integration (CON5'-F/Pvac-R), 3' integration (Hrp2-F/CON3'-R), knocked-in gene (Pfspec-F/DDimyc Rep-

R), wild type locus (Pbspec-F/PbDdiexpRm) and a control target (α6FL2–F/α6FL2-R). The PCR products were separated by agarose gel electrophoresis. The erythrocytic stage parasite lysates of wild type *P. berghei* ANKA and two PbKD clones were processed for western blotting using appropriate antibodies (mouse anti-Myc, mouse anti-HA and mouse anti-β actin for loading control), followed by HRP-conjugated goat anti-mouse IgG as described in the western blotting section.

Evaluation of PbKD parasites. The PbKD parasites were assessed for the effect of knock-down on $PfDDI_{Myc}/cDD_{HA}$ protein level, erythrocytic growth and virulence. For the effect on $PfDDI_{Myc}/cDD_{HA}$ protein level, a 2-3 months old naïve BALB/c mouse was infected intraperitoneally with a fresh stock of PbKD parasites, maintained under 70 µg/ml pyrimethamine + 40 µg/ml trimethoprim in drinking water, and the blood collected at 8-10% parasitemia. The blood was washed with FBS-RPMI medium, resuspended in FBS-RPMI medium at 2% haematocrit without or with 50 µM trimethoprim, gassed, and incubated for 12 hours at 37ºC. Parasites were purified by saponin lysis and processed for western blotting using mouse anti-HA and mouse anti-β actin (as a loading control), followed by HRP-conjugated goat anti-mouse IgG as described in the western blotting section.

For the effect of growth and virulence, 2-3 months old female BALB/c mice were infected intraperitoneally ($2x10^5$ parasites/mouse) with wild type *P. berghei* ANKA (5 mice) or PbKD parasites (10 mice). The PbKD-infected mice were divided into 2 groups of 5 mice each; one group was given 70 µg/ml pyrimethamine in drinking water (-TMP) and another group was given 70 µg/ml pyrimethamine + 40 µg/ml trimethoprim in drinking water (+TMP). Blood was collected from each mouse one day before the infection (pre-immune sera) and during later time points (days 14 and 28 of post-infection). Each mouse was monitored for infection by making Giemsa stained blood smears, parasitemia was determined by counting a minimum of 1000 cells per smear, and the data was plotted against days post-infection using the GraphPad Prism software. To determine the effect of delayed knock-down, nine female BALB/c mice were infected intraperitoneally ($2x10^5$ parasites/mouse) with PbKD parasites and given 70 µg/ml pyrimethamine + 40 µg/ml trimethoprim in drinking water. Trimethoprim was withdrawn from the drinking water of 6 mice at 5% parasitemia (-TMP), while the remaining 3 mice were given 70 µg/ml pyrimethamine + 40 µg/ml trimethoprim in drinking water (+TMP). Infection was monitored regularly by making

Giemsa stained blood smears, parasitemia was determined by counting a minimum of 1000 cells per smear, and the data was plotted against days post-infection using the GraphPad Prism software.

Challenge of recovered mice. The PbKD parasite-infected BALB/c that were never given trimethoprim (-TMP) or trimethoprim was withdrawn from the drinking water at 5% parasitemia (delayed –TMP) cleared infection. These were called recovered mice, which were monitored for almost 3 months and then challenged with wild type *P. berghei* ANKA ($2x10^5$ parasites/mouse, intraperitoneally). A group of age-matched naïve mice was also challenged similarly. Infection was monitored regularly by observing Giemsa stained blood smears, the parasitemia was determined by counting at least 1000 cells, and plotted against days post-infection using the GraphPad Prism software. 25-50 µl blood was collected from each mouse one day before the challenge (pre-challenge sera) and assessed for reactivity with parasite proteins. A group of recovered mice (4 mice) and age-matched naïve mice (5 mice) were infected with *P. yoelii* 17XNL strain (2×10^5 parasites/mouse, intra-peritoneally). Infection was monitored and data was analyzed as described above for challenge with *P. berghei* ANKA.

Immunization of mice with recombinant PbDDI1. 2-3 months old 5 female BALB/c mice were immunized intraperitoneally with emulsion of recombinant $mPbDDI_{Myc}$ (25 µg/immunization) in Freund's complete (day 0) or incomplete (days 15, 45, 75 and 105) adjuvant. A group of 5 mice was kept as a naive control and another group of 5 mice was immunized with adjuvant only. Blood was collected from each mouse for obtaining preimmune sera (day -1) and immune sera (day 30, 60, 90 and 120). The sera were assessed for reactivity against recombinant $mPbDDI_{Myc}$ by enzyme-linked immunosorbent assay (ELISA). The day 120 immune sera were pooled for each group, and assessed for the titer of anti-$mPbDDI_{Myc}$ antibodies by ELISA. Three months after the final serum collection, the immunized, naïve control and adjuvant control mice were infected intraperitoneally with wild type *P. berghei* ANKA (2×10^5 parasites/mouse), infection was monitored and data was analyzed as described above for recovered mice.

Measurement of antibody titers. The sera collected from recovered mice and immunized mice were tested for antibody titers against the soluble *P. berghei* ANKA parasite extract and recombinant $mPbDDI_{Myc}$ by ELISA, respectively. Recombinant $mPbDDI_{Myc}$ was coated on the wells of 96-well MicroWell™ MaxiSorp™ flat bottom plates (1 µg/well in 100 µl of 0.2 M bicarbonate buffer, pH 9.2) at 4°C for overnight. The plate was washed with PBS-T (PBS with

0.05% Tween 20) to remove the unbound protein, blocked (blocking solution: 2% BSA in PBS-T), and incubated with serial two-fold dilutions (in blocking solution) of sera (immune sera, adjuvant control sera and pre-immune sera) for 2 hours at room temperature. The plate was washed with PBS-T, incubated with HRP-conjugated horse anti-mouse IgG (at 1/2000 dilution in blocking solution) for 1 hour at room temperature, washed with PBS-T, and incubated with 100 µl of TMB ELISA substrate for 30 min. The reaction was stopped with 1N HCl and absorbance was measured at 450 nm using the BioTecPowerWave XS2 spectrophotometer. The absorbance values were adjusted for the background absorbance and absorbance values of the pre-immune sera. The data was plotted against the sera dilutions using the GraphPad Prism software. For antibody titers in the sera of recovered mice, a pellet of the wild type *P. berghei* ANKA erythrocytic parasites was resuspended in 5× pellet volume of the lysis buffer (PBS with 0.1% NP-40), subjected to 5 cycles of freeze-thaw, followed by 5 cycles of passage through a 27 G needle. The lysate was incubated in ice for 30 minutes and centrifuged at 25000g for 30 minutes at 4^{o}C. The supernatant that contains the soluble parasite extract was separated and the protein amount was estimated by BCA. The soluble parasite extract was coated on the wells of the 96-well MicroWell™ MaxiSorp™ flat bottom plates (2 µg protein/well in 0.2 M bicarbonate buffer, pH 9.2) and assessed for reactivity with the pre-challenge sera of recovered mice as described for recombinant mPbDDI$_{Myc}$.

Generation of DDI1 knock-down *P. falciparum* parasites. Ring stage *P. falciparum* D10 parasites were transfected with HF-pfDDIKD plasmid by electroporation as has been described earlier (74, 75). Briefly, a frozen stock of *P. falciparum* D10 was cultured to obtain ~10% early ring stage parasites. The culture was harvested, ~100 µl packed cell volume (PCV) was washed with cytomix (120 mM KCl, 0.15 mM $CaCl_2$, 2 mM EGTA, 5 mM $MgCl_2$, 10 mM $K2HPO_4/KH_2PO_4$, 25 mM HEPES, pH 7.6) and mixed with 320 µl of cytomix containing 100 µg HF-pfDDIKD plasmid DNA. The suspension was transferred to a chilled 0.2 cm electroporation cuvette and pulsed (950 µF, 310 mV, and infinite resistance) using the Bio-Rad gene pulser Xcell™. The transfected parasites were maintained and selected with 0.5 nM WR99210 till the emergence of resistant parasites. Trimethoprim was added to the culture at 10 µM when WR99210 resistant parasites reached to 5% parasitemia. The culture was harvested for isolation of genomic DNA at 3-4 weeks interval, which was used to check for plasmid integration into the target site by PCR. Primer sets specific for 5'-integration (DDi-con5U/cDD-R), 3'-integration (HRP2seq-F/DDi3'int-R), wild type locus (DDi-con5U/ DDi3'int-R) and a positive control target (PfVMP1-

Fep/PfVMP1-R) were used to determine integration at the target site. Once plasmid integration at the target site was observed, parasites were cloned by dilution cloning (76), and the clonal lines were again evaluated for plasmid DNA integration by PCR and expression of $PfDDI_{Myc}/cDD_{HA}$ protein by western blotting. For western blotting, erythrocytic stage lysates of wild type and PfDDI1 knock-down (PfKD) parasites were processed using rabbit anti-HA (at 1/1000 dilution in blocking buffer) and anti-β actin antibodies as a loading control, followed by appropriate secondary antibodies (HRP-conjugated goat anti-rabbit IgG and HRP-conjugated goat anti-mouse IgG, at 1/1000 dilution in blocking buffer) as has been described in the western blotting section.

The effect of PfDDI1 knock-down on parasite growth. The PfKD parasites were cultured in the presence of 10 μM trimethoprim and synchronized as has been described in the cell culture section. A 50 ml synchronized culture with ~10% rings was washed with RPMI1640-albumax medium, resuspended in 50 ml RPMI1640-albumax medium, and divided into two 25 ml portions. One portion was supplemented with trimethoprim and the other portion was supplemented with DMSO (0.02%). Both the portions were gassed and incubated at 37°C. After 30 hours of incubation, 20 ml of the culture was harvested from each portion (30 hour time point) and the remaining culture was expanded to 20 ml with additional medium, fresh RBCs and trimethoprim or DMSO. The cultures were gassed, incubated for 30 hours and harvested (60 hour time point). The harvested cultures were processed for isolation of parasites, which were assessed for the level of $PfDDI_{Myc}/cDD_{HA}$ by western blotting using antibodies to mouse anti-Myc and mouse anti-β actin, followed by HRP-conjugated goat anti-mouse IgG as described in the western blotting section. .

For assessment of PfDDI knock-down on erythrocytic growth, synchronized PfKD parasites were cultured for three consecutive cycles (with or without 10 μM trimethoprim), beginning with 3% parasitemia. The cultures were diluted 3-fold at the end of each cycle and fresh medium and RBCs maintain 2-3% parasitemia. Giemsa stained smears were made at various time points, total parasitemia and stages were counted in at least 1000 RBCs. The parasitemia was normalized to initial parasitemia, and plotted as fold multiplication over growth cycles using the GraphPad Prism. The percentage of ring and trophozoite/schizont stages was normalized to the total parasitemia of the respective time points, and plotted using the GraphPad Prism.

To assess the effect of DDI1 knock-down on ubiquitinated proteome of PfKD parasites, a synchronized 80 ml ring stage PfKD culture (~15% parasitemia) was divided into two halves. One

half was grown with trimethoprim and the other without trimethoprim. 30 ml of each culture was harvested at 30 hour stage (30 hour time point) and parasites were purified. Each of the remaining 10 ml cultures was expanded to 30 ml with fresh medium and RBCs, grown under the same trimethroprim condition for another 48 hours, and parasites were purified (78 hour time point). The parasite pellets were resuspended in 10× pellet volume of the lysis buffer (25 mM Tris-Cl, 10 mM KCl, 0.1 mM EDTA, 0.1 mM EGTA, 1 mM DTT, pH 7.4, 0.25% NP-40 and protease inhibitor cocktail) and incubated on ice for 30 minutes. The lysate was passed twice through a 25G needle and centrifuged at 2300g for 20 minutes at 4°C. The supernatants were processed for western blotting using mouse anti-ubiquitin (P4D1) antibodies, followed by HRP-conjugated goat anti-mouse IgG antibodies as has been described in the western blotting section.

Effect of inhibitors on PfKD parasites. The wild type *P. falciparum* D10 and PfKD parasites were compared for susceptibility to HIV protease inhibitors (lopinavir, nelfinavir and saquinavir), artemisinin, E64 and epoxomicin. For PfKD parasites, trimethoprim was maintained at 10 μM during the assay cycle (+T) or excluded during the assay cycle (-T1) or excluded in the previous cycle and during the assay cycle (-T2). For each compound, the stock was serially diluted 2-fold in 50 μl of RPMI1640-albumax medium across the wells of a 96-well tissue-culture plate. Control wells contained DMSO (0.5%) or chloroquine (500 nM). 50 μl of parasite suspension (1% ring-infected erythrocytes at 4% haematocrit) was added to each well, the plate was incubated in a modular incubator chamber (Billups-Rothenberg, Inc.) filled with the gas mixture at 37°C for 48-50 hours. At the end of incubation, the cells were fixed with 2% formaldehyde (in PBS), stained with YOYO-1 (PBS with 0.1% Triton X-100 and 10 nM YOYO-1), and the number of infected cells was determined by counting 10,000 cells using the BD Fortesa FACS Analyzer (λex 491 nm and λem 509 nm). The parasitemia of chloroquine control was subtracted from those of DMSO control and test samples to adjust for background. The adjusted parasitemias of test samples were normalized as % of the DMSO control and plotted against the concentrations of compounds to determine IC_{50} concentrations using the GraphPad Prism.

Immunoprecipitation of PfDDI1 and mass spectrometry. Asynchronous cultures of wild type *P. falciparum* D10 and PfKD (with 10 μM trimethoprim) parasites were grown and parasites were isolated at 10-15% parasitemia as has been described in the parasite culture section. The parasite pellets were resuspended in 10× pellet volume of the lysis buffer (10 mM Tris-Cl, 10 mM HEPES,

150 mm NaCl, 0.5 mM EDTA, 0.5% TritonX-100, pH 7.5; MERCK protease inhibitor cocktail), and subjected to 2 cycles of freeze-thaw, followed by passing through the 26.5 G needle. The lysates were centrifuged at 20000g for 30 min at 4°C, and the supernatant was transferred into a fresh tube. The pellet was re-extracted with 3× pellet volume of the lysis buffer as described above, and the supernatant was combined with the first supernatant. The supernatant was incubated with Myc-Trap magnetic beads (ChromoTek, 5 µl slurry/mg protein) for 2 hours at 4°C with gentle mixing. The flow through was removed and the beads were washed (10 mM Tris-Cl, 10 mM HEPES, 150 mm NaCl, 0.5 mM EDTA, pH 7.5; protease inhibitor cocktail). The beads were boiled in 100 µl of 2× SDS-PAGE sample buffer for 15 min, and the eluate was processed for western blotting and mass spectrometry. 20 µl of the eluate along with appropriate controls (input, flow through and washes) was assessed for the presence of $PfDDI_{Myc}$/cDD_{HA} by western blotting using mouse anti-Myc antibody, followed by appropriate secondary antibody as described in the western blotting section.

80 µl of the eluate was run on a 10% SDS-PAGE gel until the protein ladder completely entered into the resolving gel. The protein band was excised, cut into small pieces, treated with trypsin, peptides were extracted, vacuum dried, and resuspended in 11 µl of 2% formic acid as has been described in detail previously (77, 78). 10 µl of the peptide sample was run on the Q-Exactive HF (Thermo Fischer Scientific) for HCD mode fragmentation and LC-MS/MS analysis. The raw data files were acquired on the proteome discoverer v2.2 (Thermo Fischer Scientific), analysed and searched against the Uniprot databases of *P. falciparum* 3D7 using the HTSequest algorithm. The analysis parameters included trypsin specificity, maximum two missed cleavages and some variable modifications (carbamidomethylation of cysteine, oxidation of methionine, deamidation of asparagine/glutamine). Other parameters included: precursor tolerance of 5 ppm, fragmentation tolerance of 0.05 Da and 1% peptide FDR threshold. The protein hits from the PfKD samples were compared with those from the wild type parasites. Proteins exclusively present in the PfKD sample with at least 5 times higher peptide spectrum matches (PSMs) than in the wild type sample were selected. The selected proteins were considered if present in at least 3 biological replicates with a minimum of 1 unique peptide.

Production of recombinant *P. falciparum* pre-mRNA processing factor 19 and interaction with recombinant PfDDI1. The complete coding region of *P. falciparum* pre-mRNA processing

factor 19 (PfPRP19) was amplified from *P. falciparum* genomic DNA using primers PfPPF19-Fexp/PfPPF19-Rexp and cloned into the pGEX-6P-1 plasmid at BamHI-XhoI to obtain pGEX-PfPRP19, which was sequenced to confirm the coding region and transformed into BL21(DE3) *E. coli* cells. pGEX-PfPRP19 would express PfPRP19 as an N-terminal GST-tagged protein, facilitating purification of the recombinant $_{GST}$PfPRP19 protein using the glutathione agarose resin. A pGEX-PfPRP19 expression clone was induced with IPTG (1.0 mM) at OD_{600} of 0.6 for 12 hours at 25°C. The induced cell pellet of was resuspended in lysis buffer (PBS with 1 mg/ml lysozyme, at 5 ml/g weight of the pellet), incubated for 30 min at 4°C, sonicated using the SONICS vibra-cell Ultrasonic (5 secs pulses at 20% amplitude for 5-30 min), and centrifuged 39191g for 1 hr at 4°C. The supernatant was applied on a 1.0 ml GSTrap 4B column (GE healthcare), the column was washed with PBS, and bound proteins were eluted (50 mM Tris-Cl, 20 mM GSH, pH 8). The elutes were run on 12% SDS-PAGE, the fractions enriched with $_{GST}$PfPRP19 were concentrated (Amicon Ultra centricon: 50 kDa cut off), quantitated using BCA and used for overlay assay. Different amounts of recombinant PfDDI$_{Myc/His}$ were immobilized on nitrocellulose membrane, the membrane was blocked (3% BSA in PBST), overlaid with recombinant GST or $_{GST}$PfPRP19 (2.5 µg/ml in blocking buffer) for overnight at 4°C, and washed with blocking buffer. The membrane was incubated with mouse anti-GST antibodies, followed by HRP-conjugated goat anti-Mouse IgG as described in the western blotting section.

Effect of DNA damaging chemicals on PfDDI1 knock-down parasites and chromatin association of PfDDI. Synchronized PfKD parasites was grown with or without trimethoprim till mid trophozoite stage, supplemented with DMSO (0.005%) or DNA damaging chemicals (0.1 mM hydroxyurea and 0.0005% MMS) and grown for 6 more hours. The parasites were washed with cell culture medium, grown in fresh culture medium under the initial trimethoprim conditions for 12 hours, and total parasitemia was determined by observing Giemsa smears.

We carried out chromatin enrichment for proteomics (ChEP) to investigate association of PfDDI1 with chromatin as has been reported earlier (79, 80). A 50 ml synchronous culture of PfKD parasites (~10% parasitemia) was grown in the presence of 10 µM trimethoprim till 30 hour stage. The culture was divided into two equal parts, one part was grown with MMS (0.005% volume/volume) and the other part was grown with DMSO (0.05% volume/volume) for 6 hours. The cultures were harvested and parasites were purified as mentioned in the parasite culture

section. The parasite pellets were resuspended in 1% formaldehyde (in PBS), incubated for 10 minutes with shaking at 55 rpm and 37°C, and centrifuged 2300g. The parasite pellet was resuspended in 0.125 M glycine and incubated for 5 minutes at room temperature. The suspension was centrifuged at 2300g for 5 minutes at room temperature, the cells were washed with PBS, the parasite pellet was resuspended in 500 µl of nuclear extraction buffer (25 mM Tris-Cl, 10 mM KCl, 0.1 mM EDTA, 0.1 mM EGTA, 1 mM DTT, pH 7.4; supplemented with protease inhibitor cocktail and 0.25% NP-40), and incubated for 30 minutes in ice. The lysate was passed twice through a 25G needle, centrifuged at 2300g for 20 minutes at 4°C, and the supernatant (cytoplasm) was transferred to a microcentrifuge tube. The pellet, which contains nuclei, was resuspended in 500 µl of nuclear extraction buffer containing RNAse A (200 µg/ml) and incubated for 15 minutes at 37°C. The suspension was centrifuged at 2300g for 10 minutes at 4°C, the supernatant was discarded, and the pellet was washed twice with PBS to remove non cross-linked proteins. The pellet was resuspended in 500 µl of Tris-SDS buffer (50 mM Tris-Cl, 10 mM EDTA, pH 7.4, 4% SDS, protease inhibitor cocktail) using a hydrophobic pipette tip, and incubated for 10 minutes at room temperature. 1.5 ml of urea buffer (10 mM Tris-Cl, 1 mM EDTA, 8 M urea, pH 7.4) was added to the suspension and the sample was centrifuged at 15000g for 30 minutes at room temperature. The supernatant was discarded and the pellet was resuspended in 500 µl of Tris-SDS buffer, mixed with 1.5 ml urea buffer, and centrifuged at 15000g for 25 minutes at room temperature. The supernatant was discarded, the pellet was resuspended in 2 ml of Tris-SDS buffer, centrifuged at 15000g for 25 minutes at room temperature. The supernatant was discarded, the pellet was resuspended in 500 µl of storage buffer (10 mM Tris-Cl, 1 mM EDTA, 25 mM NaCl, 10% glycerol, pH 7.4, and protease inhibitor cocktail), and the suspension was sonicated (Diagenode Bioruptor UCD-200) at 4°C for 5 minutes to solubilize chromatin completely. The sonicated sample was centrifuged at 15000g for 30 minutes at 4°C, the supernatant containing the solubilized chromatin was transferred to a microcentrifuge tube, mixed with equal volume of SDS-PAGE sample buffer, and incubated at 98°C for 30 minutes to reverse the cross-links. The chromatin and the cytoplasmic samples were assessed for purity by western blotting using rabbit anti-Histone 2B (1/1000 diluted in blocking buffer) and rabbit anti-α2 subunit of 20S proteasome (at 1/1000 dilution in blocking buffer) antibodies, followed by appropriate secondary antibodies. Both chromatin and cytoplasmic samples were assessed for the presence of $DDI1_{Myc}/CDD_{HA}$

protein by western blot using mouse anti-Myc antibodies, followed by HRP-conjugated goat anti-mouse IgG as described in the western blotting section.

Isolation and assays with DNA-protein crosslinks. DPCs were generated and isolated from human embryonic kidney cells (HEK293T), wild type *P. falciparum* 3D7 and PfKD parasites as has been previously reported (49). HEK293T cells were cultured in DMEM (supplemented with 10% FBS, penicillin and streptomycin) at 37°C in a CO_2 incubator. The cells were treated at 70-80% confluency with 50 μM etoposide or DMSO (0.001%) and grown further for 12 hours at 37ºC in a CO_2 incubator. The culture medium was aspirated, 3 ml of the lysis buffer (5.6 M guanidine thiocyanate, 10 mM Tris-Cl, 20 mM EDTA, 4% Triton X-100, 1% sarkosyl, 1% DTT, pH 6.5) was added over the HEK293T cells (~8×10^6), and the cells were scraped off the flask. The cell suspension was mixed by pipetting using a 1 ml pipette tip and passed 6-8 times through a 24G needle. 3 ml of the chilled ethanol (-20°C) was added to the lysate and centrifuged at 21,000g for 20 minutes at 4°C. The pellet was washed twice with cold wash buffer (20 mM Tris-Cl, 150 mM NaCl, pH 6.5, 50% ethanol), solubilized in 1 ml of pre-warmed solution 1 (1% SDS, 20 mM Tris-Cl, pH 7.5) at 42°C for 6 minutes, sheared by passing 5-6 times through a 26G needle, and mixed with 1 ml of the precipitation buffer (200 mM KCl, 20 mM Tris-Cl, pH 7.5). The sample was incubated on ice for 6 min and centrifuged at 21,000g for 5 min at 4°C. The DPC pellet was washed twice with the low-salt buffer (100 mM KCl, 20 mM Tris-Cl, pH 7.5), each time by incubating at 55°C for 10 min, followed by on ice for 6 min, and centrifuged at 21,000g for 5 min at 4°C. The DPC pellet was resuspended in PBS and incubated at 37°C to solubilize. The amount of DPC-associated DNA was estimated at OD_{260}. For isolation of DPCs from the parasite, a synchronized 100 ml ring stage culture of *P. falciparum* 3D7 (~10% parasitemia) was divided into two equal parts and grown till 24 hour stage. One part was supplemented with 50 μM etoposide and another part with DMSO (0.001%). Both the cultures were grown for another 10 hours, parasites were purified and processed for isolation of DPCs as has been described for HEK293T cells.

We assessed PfKD parasites for the presence of DPCs and the association of PfDDI1 with DPCs. A synchronized 140 ml ring stage culture of PfKD parasites (~15% parasitemia) was divided into two equal parts. One part was grown with trimethoprim (10 μM) and another without trimethoprim. 50 ml of each culture was harvested at 30 hour stage (30 hour time point) and parasites were purified. The remaining 20 ml culture was expanded to 50 ml with fresh medium

and RBCs, grown under the same trimethoprim condition for another 48 hours, and the parasites were purified (78 hour time point). The parasite pellets were processed for isolation of DPCs and DPC-associated DNA. DPCs were isolated as has been described for HEK293T cells. For DPC-associated DNA, parasites were processed upto the precipitation step (precipitation with 200 mM KCl, 20 mM Tris-Cl, pH 7.5) as has been described for HEK293T cells. After precipitation, the supernatant was processed for isolation of free DNA and the pellet was processed for isolation of DPC-associated DNA. The DPC pellet was washed twice, each time with 1.5 ml of the low-salt buffer (100 mM KCl, 20 mM Tris-Cl, pH 7.5) by incubating at 55°C for 10 min, followed by on ice for 6 min, and centrifuged at 21,000g at 4°C for 5 min. The washes were pooled with the supernatant from the precipitation step. The DPC pellet was resuspended in 1 ml of proteinase K buffer (100 mM KCl, 20 mM Tris-Cl, pH 7.5 and 10 mM EDTA, proteinase K at 0.2 mg/ml), incubated at 55°C for 45 min, followed by on ice for 6 min. The sample was centrifuged at 21000g for 10 min at 4°C, the pellet (debris and proteins released from the digestion of DPCs) was discarded and the supernatant that contains the DPC-associated DNA was retained. The amount of DNA in DPC-associated DNA sample (supernatant of the proteinase K digested sample) and DPC-free DNA sample (pooled supernatant and washes) was quantitated using the SYBR green dye as per the manufacturer's instructions. The amount of DPC-associated DNA was expressed as the percentage of total DNA (DNA present in the DPC sample and DPC-free DNA sample). For detection of DPC-associated PfDDI1, the 78 hour time point DPC preparations were spotted on a nitrocellulose membrane. The membrane was blocked (3% BSA in TBST), incubated with mouse anti-HA antibodies, followed by HRP-conjugated goat anti-mouse IgG antibodies, and signal was developed as has been described in the western blotting section.

We assessed DPCs for interaction with recombinant PfDDI1. DPC preparations from the DMSO-treated and etoposide-treated wild type *P. falciparum* 3D7 parasites and HEK293T cells were spotted on a nitrocellulose membrane, and the membrane was blocked (3% BSA in TBST). The membranes with HEK293T DPC spots were assessed for the presence of DPCs of topoisomerase II and histone 2B (as a chromatin control) using antibodies to rabbit human topoisomerase II and rabbit anti-H2B, followed by HRP-conjugated goat anti-rabbit IgG. For interaction of recombinant PfDDI1 with DPCs, pure parasite genomic DNA was also spotted as a control along with the wild type *P. falciparum* DPC preparations. These membranes were overlaid with purified recombinant $PfDDI1_{Myc/His}$ (2.5 µg/ml in blocking buffer) for 12-14 hours at 4°C,

washed with blocking buffer, incubated with rabbit anti-His antibodies, washed with blocking buffer and then with HRP-conjugated goat anti-rabbit IgG antibodies. The blots were developed as has been described in the western blotting section.

Complementation of *S. cerevisiae* DDI1. The ScDDI1 coding region of *S. cerevisiae* BY4741strain was replaced with kanamycin cassette (for knock-out) or the GFP-PfDDI1$_{Myc}$ cassette containing the wild type or mutant PfDDI1 coding sequence (knock-in). The kanamycin cassette was amplified from pFA6a-kanMX6 plasmid using ScDDi-Fko/PfDDi-Rki primers. For wild type PfDDI transfection cassette, the pGEX-synPfDDI$_{Myc}$ plasmid was digested with XhoI, ends were filled with Klenow, and again digested with BamHI to excise the PfDDI1$_{Myc}$ region, which was cloned into the pFA6a-GFP plasmid at BamHI/SmaI site to obtain the pFA6-GFP/PfDDI$_{Myc}$ plasmid. The plasmid was used as a template for PCR amplification of the wild type PfDDI1 transfection cassette (GFP/wPfDDI$_{Myc}$) using PfDDi-Fki/PfDDi-Rki primers. The mutant PfDDI transfection cassette (GFP/wPfDDI$_{Myc}$) was generated by recombination PCR using the pFA6-GFP/PfDDI$_{Myc}$ plasmid as a template with PfDDi-Fki/PRPsynD-A-R and PRPsynD-A-F/PfDDi-Rki primer sets as described for recombinant mPbDDI1$_{Myc}$ in the production of recombinant proteins section. The kanamycin cassette, GFP/wPfDDI$_{Myc}$ and GFP/mPfDDI$_{Myc}$ PCR products were gel purified and transformed into the BY4741 cells by lithium acetate method (81). Briefly, the BY4741 strain was grown in complete YPD medium at 25ºC and 250 rpm till OD_{600} of 1.0. The culture was centrifuged (3000g for 5 minutes at 25ºC), the cell pellet was washed with autoclaved Milli-Q water, followed by with lithium acetate/Tris EDTA (LTE) buffer (100 mM lithium acetate, 10 mM Tris-Cl, 4 mM EDTA, pH 7.5). The cell pellet was resuspended in 100 µl of transformation mix (LTE, 34.7% PEG, 10 µg of calf thymus DNA, 4 µg of desired PCR product), incubated at 30°C for one hour, followed by at 42ºC for 15 minutes, and then in ice for 10 minutes. The transformation reaction was centrifuged at 3300g for 2 minutes at room temperature, the cell pellet was resuspended in YPD medium, and grown at 25°C with shaking at 250 rpm for overnight. The culture was centrifuged at 3000g for 5 minutes at room temperature, the cell pellet was washed with autoclaved Milli-Q water, resuspended in autoclaved Milli-Q water, spread on YPD agarose plates containing G418 (350 µg/ml), and the plates were incubated at 25ºC. The resistant colonies along with the BY4741strain as a control were grown overnight in 5 ml of YPD medium at 25ºC and 250 rpm. The cultures were harvested at 3000g for 5 minutes at 25ºC, and the cell pellets were used for western blot analysis and gDNA isolation as has been

described earlier (78). The integration of transfection cassette was checked by PCR using primers specific for the complete cassette (Sc/PfDDi-5con, Sc/PfDDi-3con), 5'-integration (Sc/PfDDi-5con and PfDDIUbl-R) and 3'-integration (RVP/UBA-F and Sc/pfDDi 3con) loci. The lysates of complemented (ΔScddi :: wPfDDI1$_{Myc}$ and ΔScDDI1 :: mPfDDI1$_{Myc}$) strains and BY4741 as a control were evaluated for expression of GFP/wPfDDI$_{Myc}$ or GFP/mPfDDI$_{Myc}$ proteins by western blotting using anti-GFP antibodies and anti-triose phosphate isomerase antibodies, followed by appropriate secondary antibodies as has been described in western blotting section.

The BY4741, ΔScDDI1 and complemented (ΔScddi :: wPfDDI1$_{Myc}$ and ΔScDDI1 :: mPfDDI1$_{Myc}$) strains were compared for growth on YPD agarose plate containing various inhibitors. In brief, overnight cultures were initiated with single colonies in complete YPD with G418 (for complemented strains) at 25ºC and 250 rpm. The overnight culture was added to fresh complete YPD medium (at 1%) without G418, and grown till the OD_{600} of 1-2. The cultures were normalized to OD_{600} of 1.0, serial 10-fold dilutions were made in YPD, and 5 µl of each dilution of all the strains was spotted on YPD agarose plates without or with a test chemical (0.005% MMS, 100 µg/ml etoposide, 100 mM hydroxyurea, 0.1% glyoxal, 100 µM artemisnin, 100 µM chloroquine, 100 µM pepstatin A, 100 µM bestatin, 100 µM lopinavir and 100 µM nelfinavir). The plates were incubated at 30°C for 2-3 days.

The BY4741, ΔScDDI1 and complemented (ΔScddi :: wPfDDI1$_{Myc}$) strains were compared for protein secretion into the culture medium. For each strain, a single colony was inoculated into 5 ml SD medium, incubated at 30ºC for 48 hours with shaking at 180 rpm, and the culture was centrifuged at 3000g for 15 minutes at 25ºC. The cell pellet was dried at 100°C for overnight and the pellet weight was measured. The supernatant was dialysed against PBS at 4°C using a 3.5 kDa cut off dialysis membrane and the protein amount was estimated using BCA method. The total protein amount present in the supernatant was normalized with dry weight of the cell pellet from the same culture and plotted as µg/mg dry weight of the pellet using GraphPad Prism.

ACKNOWLEDGEMENTS

This study and the salaries of MAN, NA and AKN were supported by funding from the Department of Biotechnology, India (grant reference numbers: 102/IFD/SAN/2914/2015-2016 and BT/PR11497/MED/29/854/2014). NT and KS are recipients of Research Fellowship from CSIR, India. RS and ZR were supported by fellowships from DBT. The authors would like to acknowledge CCMB central microscopy, Animal and proteomics facilities for their technical support.

AUTHOR CONTRIBUTIONS

NT, MAN, NA and PSS conceived the project, designed experiments, interpreted the results and wrote the manuscript. NT, MAN and NA carried out the majority of experiments. KS, ZR and RS carried out experiments related to parasite growth, DPC and complementation in yeast. and cloning experiments. RP guided NA for *S. cerevisiae* experiments. Atul carried out experiments related to generation of PfDDI1 antiserum and localization in *P. falciparum*. FMAA and KAK carried out experiments related to *P. berghei* sporozoite and liver stages. KAK contributed to manuscript writing.

Competing interests

The author(s) declare no competing interests.

REFERENCES

1. Livneh I, Cohen-Kaplan V, Cohen-Rosenzweig C, Avni N, Ciechanover A. 2016. The life cycle of the 26S proteasome: from birth, through regulation and function, and onto its death. Cell Res 26:869-85.
2. Goldberg AL. 2005. Nobel Committee Tags Ubiquitin for Distinction. Neuron 45:339-344.
3. Gantt SM, Myung JM, Briones MR, Li WD, Corey EJ, Omura S, Nussenzweig V, Sinnis P. 1998. Proteasome inhibitors block development of Plasmodium spp. Antimicrob Agents Chemother 42:2731-8.
4. Lindenthal C, Weich N, Chia YS, Heussler V, Klinkert MQ. 2005. The proteasome inhibitor MLN-273 blocks exoerythrocytic and erythrocytic development of Plasmodium parasites. Parasitology 131:37-44.
5. Czesny B, Goshu S, Cook JL, Williamson KC. 2009. The Proteasome Inhibitor Epoxomicin Has Potent Plasmodium falciparum Gametocytocidal Activity. Antimicrobial Agents and Chemotherapy 53:4080-4085.
6. Ng CL, Fidock DA, Bogyo M. 2017. Protein Degradation Systems as Antimalarial Therapeutic Targets. Trends in parasitology 33:731-743.
7. Wyllie S, Brand S, Thomas M, De Rycker M, Chung C-w, Pena I, Bingham RP, Bueren-Calabuig JA, Cantizani J, Cebrian D, Craggs PD, Ferguson L, Goswami P, Hobrath J, Howe J, Jeacock L, Ko E-J, Korczynska J, MacLean L, Manthri S, Martinez MS, Mata-Cantero L, Moniz S, Nühs A, Osuna-Cabello M, Pinto E, Riley J, Robinson S, Rowland P, Simeons FRC, Shishikura Y, Spinks D, Stojanovski L, Thomas J, Thompson S, Viayna Gaza E, Wall RJ, Zuccotto F, Horn D, Ferguson MAJ, Fairlamb AH, Fiandor JM, Martin J, Gray DW, Miles TJ, Gilbert IH, Read KD, Marco M, Wyatt PG. 2019. Preclinical candidate for the treatment of visceral leishmaniasis that acts through proteasome inhibition. Proceedings of the National Academy of Sciences 116:9318-9323.
8. Li H, O'Donoghue AJ, van der Linden WA, Xie SC, Yoo E, Foe IT, Tilley L, Craik CS, da Fonseca PCA, Bogyo M. 2016. Structure- and function-based design of Plasmodium-selective proteasome inhibitors. Nature 530:233-236.
9. Khare S, Nagle AS, Biggart A, Lai YH, Liang F, Davis LC, Barnes SW, Mathison CJN, Myburgh E, Gao M-Y, Gillespie JR, Liu X, Tan JL, Stinson M, Rivera IC, Ballard J, Yeh V, Groessl T, Federe G, Koh HXY, Venable JD, Bursulaya B, Shapiro M, Mishra PK, Spraggon G, Brock A, Mottram JC, Buckner FS, Rao SPS, Wen BG, Walker JR, Tuntland T, Molteni V, Glynne RJ, Supek F. 2016. Proteasome inhibition for treatment of leishmaniasis, Chagas disease and sleeping sickness. Nature 537:229-233.
10. Hershko A, Ciechanover A. 1982. Mechanisms of intracellular protein breakdown. Annu Rev Biochem 51:335-64.
11. Ciechanover A. 2009. Tracing the history of the ubiquitin proteolytic system: the pioneering article. Biochem Biophys Res Commun 387:1-10.
12. Saeki Y. 2017. Ubiquitin recognition by the proteasome. J Biochem 161:113-124.
13. Finley D. 2009. Recognition and processing of ubiquitin-protein conjugates by the proteasome. Annu Rev Biochem 78:477-513.
14. Sirkis R, Gerst JE, Fass D. 2006. Ddi1, a eukaryotic protein with the retroviral protease fold. J Mol Biol 364:376-87.
15. Liu Y, Xiao W. 1997. Bidirectional regulation of two DNA-damage-inducible genes, MAG1 and DDI1, from Saccharomyces cerevisiae. Mol Microbiol 23:777-89.
16. Lustgarten V, Gerst JE. 1999. Yeast VSM1 encodes a v-SNARE binding protein that may act as a negative regulator of constitutive exocytosis. Mol Cell Biol 19:4480-94.
17. Marash M, Gerst JE. 2003. Phosphorylation of the autoinhibitory domain of the Sso t-SNAREs promotes binding of the Vsm1 SNARE regulator in yeast. Mol Biol Cell 14:3114-25.
18. Gabriely G, Kama R, Gelin-Licht R, Gerst JE. 2008. Different domains of the UBL-UBA ubiquitin receptor, Ddi1/Vsm1, are involved in its multiple cellular roles. Mol Biol Cell 19:3625-37.
19. White RE, Dickinson JR, Semple CA, Powell DJ, Berry C. 2011. The retroviral proteinase active site and the N-terminus of Ddi1 are required for repression of protein secretion. FEBS Lett 585:139-42.
20. Clarke DJ, Mondesert G, Segal M, Bertolaet BL, Jensen S, Wolff M, Henze M, Reed SI. 2001. Dosage suppressors of pds1 implicate ubiquitin-associated domains in checkpoint control. Mol Cell Biol 21:1997-2007.
21. Kaplun L, Tzirkin R, Bakhrat A, Shabek N, Ivantsiv Y, Raveh D. 2005. The DNA damage-inducible UbL-UbA protein Ddi1 participates in Mec1-mediated degradation of Ho endonuclease. Mol Cell Biol 25:5355-62.

22. Voloshin O, Bakhrat A, Herrmann S, Raveh D. Transfer of Ho endonuclease and Ufo1 to the proteasome by the UbL-UbA shuttle protein, Ddi1, analysed by complex formation in vitro. PLoS One 7:e39210.
23. Ivantsiv Y, Kaplun L, Tzirkin-Goldin R, Shabek N, Raveh D. 2006. Unique Role for the UbL-UbA Protein Ddi1 in Turnover of SCF^{Ufo1} Complexes. Molecular and Cellular Biology 26:1579-1588.
24. Trempe JF, Brown NR, Lowe ED, Gordon C, Campbell ID, Noble ME, Endicott JA. 2005. Mechanism of Lys48-linked polyubiquitin chain recognition by the Mud1 UBA domain. Embo j 24:3178-89.
25. Ramirez J, Lectez B, Osinalde N, Sivá M, Elu N, Aloria K, Procházková M, Perez C, Martínez-Hernández J, Barrio R, Šašková KG, Arizmendi JM, Mayor U. 2018. Quantitative proteomics reveals neuronal ubiquitination of Rngo/Ddi1 and several proteasomal subunits by Ube3a, accounting for the complexity of Angelman syndrome. Human Molecular Genetics 27:1955-1971.
26. Serbyn N, Noireterre A, Bagdiul I, Plank M, Michel AH, Loewith R, Kornmann B, Stutz F. 2020. The Aspartic Protease Ddi1 Contributes to DNA-Protein Crosslink Repair in Yeast. Mol Cell 77:1066-1079.e9.
27. Svoboda M, Konvalinka J, Trempe J-F, Saskova KG. 2019. The yeast proteases Ddi1 and Wss1 are both involved in the DNA replication stress response doi:10.1101/584508. bioRxiv.
28. Morawe T, Honemann-Capito M, von Stein W, Wodarz A. Loss of the extraproteasomal ubiquitin receptor Rings lost impairs ring canal growth in Drosophila oogenesis. J Cell Biol 193:71-80.
29. Lehrbach NJ, Ruvkun G. 2016. Proteasome dysfunction triggers activation of SKN-1A/Nrf1 by the aspartic protease DDI-1. eLife 5:e17721.
30. Koizumi S, Irie T, Hirayama S, Sakurai Y, Yashiroda H, Naguro I, Ichijo H, Hamazaki J, Murata S. 2016. The aspartyl protease DDI2 activates Nrf1 to compensate for proteasome dysfunction. Elife 5.
31. Yip MCJ, Bodnar NO, Rapoport TA. 2020. Ddi1 is a ubiquitin-dependent protease. Proc Natl Acad Sci U S A 117:7776-7781.
32. Dirac-Svejstrup AB, Walker J, Faull P, Encheva V, Akimov V, Puglia M, Perkins D, Kümper S, Hunjan SS, Blagoev B, Snijders AP, Powell DJ, Svejstrup JQ. 2020. DDI2 Is a Ubiquitin-Directed Endoprotease Responsible for Cleavage of Transcription Factor NRF1. Molecular Cell doi:https://doi.org/10.1016/j.molcel.2020.05.035.
33. Trempe JF, Šašková KG, Sivá M, Ratcliffe CD, Veverka V, Hoegl A, Ménade M, Feng X, Shenker S, Svoboda M, Kožíšek M, Konvalinka J, Gehring K. 2016. Structural studies of the yeast DNA damage-inducible protein Ddi1 reveal domain architecture of this eukaryotic protein family. Sci Rep 6:33671.
34. Sivá M, Svoboda M, Veverka V, Trempe JF, Hofmann K, Kožíšek M, Hexnerová R, Sedlák F, Belza J, Brynda J, Šácha P, Hubálek M, Starková J, Flaisigová I, Konvalinka J, Šašková KG. 2016. Human DNA-Damage-Inducible 2 Protein Is Structurally and Functionally Distinct from Its Yeast Ortholog. Sci Rep 6:30443.
35. Kumar S, Suguna K. 2018. Crystal structure of the retroviral protease-like domain of a protozoal DNA damage-inducible 1 protein. FEBS Open Bio 8:1379-1394.
36. Nowicka U, Zhang D, Walker O, Krutauz D, Castañeda CA, Chaturvedi A, Chen TY, Reis N, Glickman MH, Fushman D. 2015. DNA-damage-inducible 1 protein (Ddi1) contains an uncharacteristic ubiquitin-like domain that binds ubiquitin. Structure 23:542-557.
37. White RE, Powell DJ, Berry C. 2011. HIV proteinase inhibitors target the Ddi1-like protein of Leishmania parasites. Faseb j 25:1729-36.
38. White RE, Powell DJ, Berry C. HIV proteinase inhibitors target the Ddi1-like protein of Leishmania parasites. FASEB J 25:1729-36.
39. Zhang H, Liu J, Ying Z, Li S, Wu Y, Liu Q. 2020. Toxoplasma gondii UBL-UBA shuttle proteins contribute to the degradation of ubiquitinylated proteins and are important for synchronous cell division and virulence. Faseb j 34:13711-13725.
40. Parikh S, Gut J, Istvan E, Goldberg DE, Havlir DV, Rosenthal PJ. 2005. Antimalarial activity of human immunodeficiency virus type 1 protease inhibitors. Antimicrob Agents Chemother 49:2983-5.
41. Skinner-Adams TS, McCarthy JS, Gardiner DL, Hilton PM, Andrews KT. 2004. Antiretrovirals as antimalarial agents. J Infect Dis 190:1998-2000.
42. Hobbs CV, Voza T, Coppi A, Kirmse B, Marsh K, Borkowsky W, Sinnis P. 2009. HIV protease inhibitors inhibit the development of preerythrocytic-stage plasmodium parasites. J Infect Dis 199:134-41.
43. Hobbs CV, Tanaka TQ, Muratova O, Van Vliet J, Borkowsky W, Williamson KC, Duffy PE. 2013. HIV treatments have malaria gametocyte killing and transmission blocking activity. J Infect Dis 208:139-48.
44. Nsanzabana C, Rosenthal PJ. 2011. In vitro activity of antiretroviral drugs against Plasmodium falciparum. Antimicrobial agents and chemotherapy 55:5073-5077.

45. Achan J, Kakuru A, Ikilezi G, Ruel T, Clark TD, Nsanzabana C, Charlebois E, Aweeka F, Dorsey G, Rosenthal PJ, Havlir D, Kamya MR. 2012. Antiretroviral agents and prevention of malaria in HIV-infected Ugandan children. N Engl J Med 367:2110-8.
46. Wlodawer A, Erickson JW. 1993. Structure-based inhibitors of HIV-1 protease. Annu Rev Biochem 62:543-85.
47. Perteguer MJ, Gómez-Puertas P, Cañavate C, Dagger F, Gárate T, Valdivieso E. 2013. Ddi1-like protein from Leishmania major is an active aspartyl proteinase. Cell Stress Chaperones 18:171-81.
48. Nsanzabana C, Rosenthal PJ. 2011. In vitro activity of antiretroviral drugs against Plasmodium falciparum. Antimicrob Agents Chemother 55:5073-7.
49. Hu Q, Klages-Mundt N, Wang R, Lynn E, Kuma Saha L, Zhang H, Srivastava M, Shen X, Tian Y, Kim H, Ye Y, Paull T, Takeda S, Chen J, Li L. 2020. The ARK Assay Is a Sensitive and Versatile Method for the Global Detection of DNA-Protein Crosslinks. Cell Reports 30:1235-1245.e4.
50. Bertolaet BL, Clarke DJ, Wolff M, Watson MH, Henze M, Divita G, Reed SI. 2001. UBA domains mediate protein-protein interactions between two DNA damage-inducible proteins. J Mol Biol 313:955-63.
51. Bertolaet BL, Clarke DJ, Wolff M, Watson MH, Henze M, Divita G, Reed SI. 2001. UBA domains of DNA damage-inducible proteins interact with ubiquitin. Nat Struct Biol 8:417-22.
52. Mahajan K. 2016. hPso4/hPrp19: a critical component of DNA repair and DNA damage checkpoint complexes. Oncogene 35:2279-86.
53. Yin J, Zhu JM, Shen XZ. 2012. New insights into pre-mRNA processing factor 19: A multi-faceted protein in humans. Biol Cell 104:695-705.
54. De Cesare V, Carbajo Lopez D, Mabbitt PD, Fletcher AJ, Soetens M, Antico O, Wood NT, Virdee S. 2021. Deubiquitinating enzyme amino acid profiling reveals a class of ubiquitin esterases. Proceedings of the National Academy of Sciences 118:e2006947118.
55. McClellan AJ, Laugesen SH, Ellgaard L. 2019. Cellular functions and molecular mechanisms of non-lysine ubiquitination. Open Biol 9:190147.
56. Ting LM, Gissot M, Coppi A, Sinnis P, Kim K. 2008. Attenuated Plasmodium yoelii lacking purine nucleoside phosphorylase confer protective immunity. Nat Med 14:954-8.
57. Spaccapelo R, Aime E, Caterbi S, Arcidiacono P, Capuccini B, Di Cristina M, Dottorini T, Rende M, Bistoni F, Crisanti A. 2011. Disruption of plasmepsin-4 and merozoites surface protein-7 genes in Plasmodium berghei induces combined virulence-attenuated phenotype. Sci Rep 1:39.
58. Spaccapelo R, Janse CJ, Caterbi S, Franke-Fayard B, Bonilla JA, Syphard LM, Di Cristina M, Dottorini T, Savarino A, Cassone A, Bistoni F, Waters AP, Dame JB, Crisanti A. 2010. Plasmepsin 4-deficient Plasmodium berghei are virulence attenuated and induce protective immunity against experimental malaria. Am J Pathol 176:205-17.
59. Aly AS, Downie MJ, Mamoun CB, Kappe SH. 2010. Subpatent infection with nucleoside transporter 1-deficient Plasmodium blood stage parasites confers sterile protection against lethal malaria in mice. Cell Microbiol 12:930-8.
60. Bridgford JL, Xie SC, Cobbold SA, Pasaje CFA, Herrmann S, Yang T, Gillett DL, Dick LR, Ralph SA, Dogovski C, Spillman NJ, Tilley L. 2018. Artemisinin kills malaria parasites by damaging proteins and inhibiting the proteasome. Nature Communications 9:3801.
61. Schmidtke G, Holzhütter HG, Bogyo M, Kairies N, Groll M, de Giuli R, Emch S, Groettrup M. 1999. How an inhibitor of the HIV-I protease modulates proteasome activity. J Biol Chem 274:35734-40.
62. Brüning A, Burger P, Vogel M, Rahmeh M, Gingelmaiers A, Friese K, Lenhard M, Burges A. 2009. Nelfinavir induces the unfolded protein response in ovarian cancer cells, resulting in ER vacuolization, cell cycle retardation and apoptosis. Cancer Biol Ther 8:226-32.
63. Kraus M, Malenke E, Gogel J, Müller H, Rückrich T, Overkleeft H, Ovaa H, Koscielniak E, Hartmann JT, Driessen C. 2008. Ritonavir induces endoplasmic reticulum stress and sensitizes sarcoma cells toward bortezomib-induced apoptosis. Mol Cancer Ther 7:1940-8.
64. Jiang W, Mikochik PJ, Ra JH, Lei H, Flaherty KT, Winkler JD, Spitz FR. 2007. HIV protease inhibitor nelfinavir inhibits growth of human melanoma cells by induction of cell cycle arrest. Cancer Res 67:1221-7.
65. Boddey JA, Hodder AN, Günther S, Gilson PR, Patsiouras H, Kapp EA, Pearce JA, de Koning-Ward TF, Simpson RJ, Crabb BS, Cowman AF. 2010. An aspartyl protease directs malaria effector proteins to the host cell. Nature 463:627-31.
66. Russo I, Babbitt S, Muralidharan V, Butler T, Oksman A, Goldberg DE. 2010. Plasmepsin V licenses Plasmodium proteins for export into the host erythrocyte. Nature 463:632-6.

67. Ridewood S, Dirac-Svejstrup AB, Howell S, Weston A, Lehmann C, Patel AP, Collinson L, Bingham R, Powell D, Snijder A, Svejstrup JQ, Deu E. 2021. The Aspartyl Protease Ddi1 Is Essential for Erythrocyte Invasion by the Malaria Parasite. bioRxiv doi:10.1101/2021.05.11.443575:2021.05.11.443575.
68. Onchieku NM, Kumari S, Pandey R, Sharma V, Kumar M, Deshmukh A, Kaur I, Mohmmed A, Gupta D, Kiboi D, Gaur N, Malhotra P. 2021. Artemisinin acts by inhibiting Plasmodium falciparum Ddi1, a retropepsin, resulting into the accumulation of ubiquitinated proteins. bioRxiv doi:10.1101/2021.07.12.452004:2021.07.12.452004.
69. Lambros C, Vanderberg JP. 1979. Synchronization of Plasmodium falciparum erythrocytic stages in culture. J Parasitol 65:418-20.
70. Fivelman QL, McRobert L, Sharp S, Taylor CJ, Saeed M, Swales CA, Sutherland CJ, Baker DA. 2007. Improved synchronous production of Plasmodium falciparum gametocytes in vitro. Mol Biochem Parasitol 154:119-23.
71. Singhal N, Atul, Mastan BS, Kumar KA, Sijwali PS. Genetic ablation of plasmoDJ1, a multi-activity enzyme, attenuates parasite virulence and reduces oocyst production. Biochem J 461:189-203.
72. Navale R, Atul, Allanki AD, Sijwali PS. Characterization of the autophagy marker protein Atg8 reveals atypical features of autophagy in Plasmodium falciparum. PLoS One 9:e113220.
73. Al-Nihmi FM, Kolli SK, Reddy SR, Mastan BS, Togiri J, Maruthi M, Gupta R, Sijwali PS, Mishra S, Kumar KA. 2017. A Novel and Conserved Plasmodium Sporozoite Membrane Protein SPELD is Required for Maturation of Exo-erythrocytic Forms. Sci Rep 7:40407.
74. Fidock DA, Wellems TE. 1997. Transformation with human dihydrofolate reductase renders malaria parasites insensitive to WR99210 but does not affect the intrinsic activity of proguanil. Proc Natl Acad Sci U S A 94:10931-6.
75. Govindarajalu G, Rizvi Z, Kumar D, Sijwali PS. 2019. Lyse-Reseal Erythrocytes for Transfection of Plasmodium falciparum. Sci Rep 9:19952.
76. Sijwali PS, Koo J, Singh N, Rosenthal PJ. 2006. Gene disruptions demonstrate independent roles for the four falcipain cysteine proteases of Plasmodium falciparum. Mol Biochem Parasitol 150:96-106.
77. Sudhakar R, Das D, Thanumalayan S, Gorde S, Sijwali PS. 2021. Plasmodium falciparum Atg18 localizes to the food vacuole via interaction with the multi-drug resistance protein 1 and phosphatidylinositol 3-phosphate. Biochem J 478:1705-1732.
78. Bhattacharjee M, Adhikari N, Sudhakar R, Rizvi Z, Das D, Palanimurugan R, Sijwali PS. 2020. Characterization of Plasmodium falciparum NEDD8 and identification of cullins as its substrates. Sci Rep 10:20220.
79. Batugedara G, Lu XM, Saraf A, Sardiu ME, Cort A, Abel S, Prudhomme J, Washburn MP, Florens L, Bunnik EM, Le Roch KG. 2020. The chromatin bound proteome of the human malaria parasite. Microb Genom 6.
80. Kustatscher G, Hégarat N, Wills KLH, Furlan C, Bukowski-Wills J-C, Hochegger H, Rappsilber J. 2014. Proteomics of a fuzzy organelle: interphase chromatin. The EMBO Journal 33:648-664.
81. Janke C, Magiera MM, Rathfelder N, Taxis C, Reber S, Maekawa H, Moreno-Borchart A, Doenges G, Schwob E, Schiebel E, Knop M. 2004. A versatile toolbox for PCR-based tagging of yeast genes: new fluorescent proteins, more markers and promoter substitution cassettes. Yeast 21:947-62.

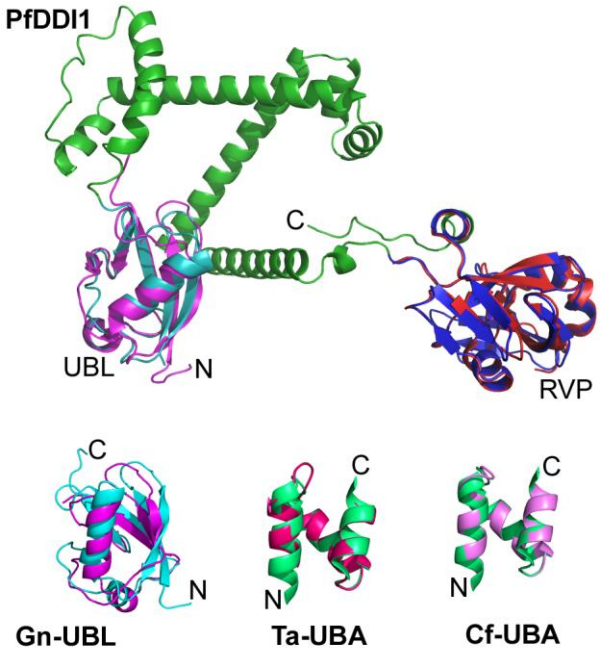

Figure S1. Domain structures of PfDDI1 and other apicomplexan DDI1 proteins. The AlphaFold structure of PfDDI1 (AF-Q8IM03-F1) shows putative UBL (cyan) and RVP (blue)) domains that are superimposed with the reported structures of ScDDI1 UBL (magenta) and RVP (red) domains. The *Gregarina niphandrodes* UBL (Gn-UBL, 2-70), *Theileria annulata* UBA (Ta-UBA, 367-403) and *Cytauxzoon felis* UBA (Cf-UBA, 354-393) domains were predicted by homology modeling. The modelled structures of Gn-UBL (cyan) was superimposed on the reported structure of ScDDI1 UBL (magenta). The modelled structures of Ta-UBA (pink) and Cf-UBA (purple) were superimposed on the reported structure of *Schizosaccharomyces pombe* DDI1 UBA domain (green). N and C are for N- and C-termini, respectively.

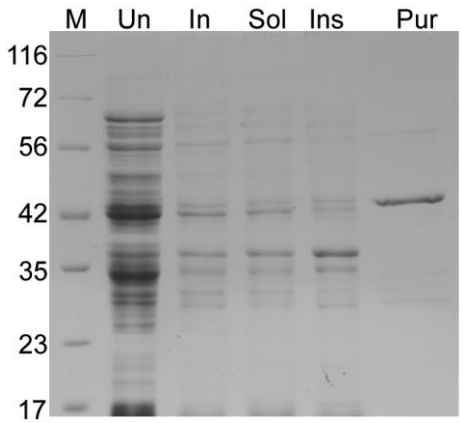

Figure S2. Production of recombinant PfDDI1. The native PfDDI1 coding region was expressed as a N-terminal His-tagged protein in *E. coli* M15(pREP4) cells using the pQE30 plasmid. The recombinant protein was purified from IPTG-induced cells by Ni-NTA chromatography under denaturing conditions and refolded. The lysates of uninduced (Un) and induced (In) cells, soluble (Sol) and insoluble (Ins) fractions of induced cells, and refolded protein (Pur) were run on SDS-PAGE gel and visualized by coomassie staining. The sizes of proteins markers (M) are indicated in kDa.

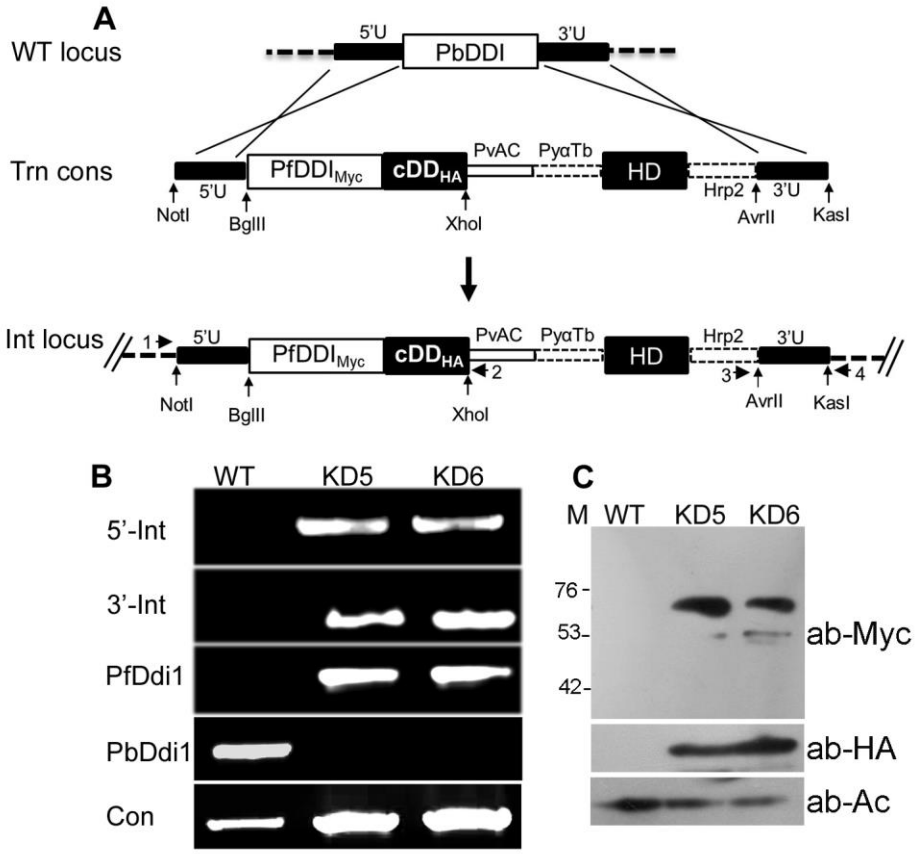

Figure S3. Generation of DDI1 knock-down *P. berghei* parasites. The endogenous PbDDI1 coding region was replaced with PfDDI1$_{Myc}$/cDD$_{HA}$ coding sequence, and cloned parasites were assessed for the presence of knock-down locus by PCR and expression of PfDDI1$_{Myc}$/cDD$_{HA}$ protein by westen blotting. **A.** The schematic represents integration of linear transfection construct (Trn cons) into the endogenous PbDDI1 locus (WT locus), resulting into the generation of integration locus (Int locus). Rectangular boxes represent the coding regions for PbDDI1 (PbDDI), PfDDI1 (PfDDI) cDD$_{HA}$ and hDHFR (HD). The flanking untranslated regions (5′U and 3′U), the location and orientation of primers (horizontal arrows), the restriction endonuclease sites (vertical arrows), and regulatory regions in the linear transfection construct (3′U of PvAC, 5′U of PyαTb, 3′U of PfHrp2) are indicated. Locus specific primers (5' integration, 5'-Int (1/2); 3' integration, 3'-Int (3/4); wild type locus, WTsp (1/4); proteasome α-6 gene as a control, Con) were used to differentiate the integration and wild type loci by PCR. **B.** The ethidium bromide stained agarose gel shows PCR products for the indicated regions from the genomic DNAs of wild type (WT) and knock-down (KD5 and KD6) parasites. **C.** The western blot of WT and knock-down (KD5 and KD6) parasite lysates was probed with antibodies to Myc (ab-Myc), HA (ab-HA) or β-actin (ab-Ac).

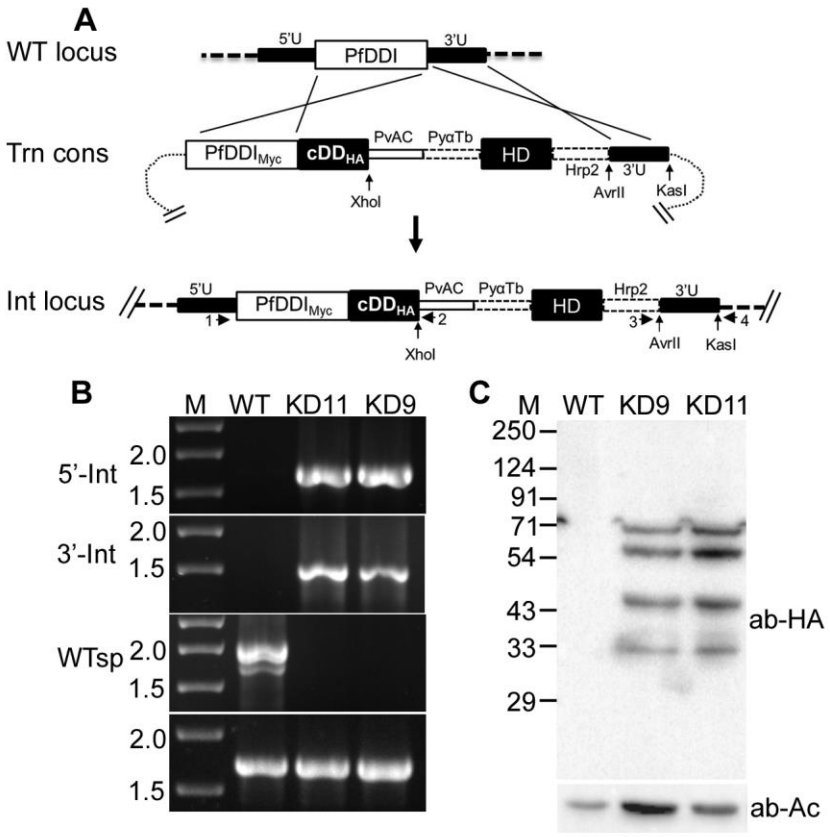

Figure S4. Generation of DDI1 knock-down *P. falciparum* parasites. The wild type PfDDI1 coding region was replaced with PfDDI1$_{Myc}$/cDD$_{HA}$ coding sequence, and the recombinant parasites were assessed for the presence of knock-down locus by PCR and expression of PfDDI1$_{Myc}$/cDD$_{HA}$ protein by western blotting. **A.** The schematic represents integration of transfection construct (Trn cons) into the endogenous PfDDI1 locus (WT locus) via double homologous crossover, resulting into the generation of integration locus (Int locus). Rectangular boxes represent the coding regions for PfDDI1 (PfDDI), PfDDI1$_{Myc}$ (PfDDI$_{Myc}$), cDD$_{HA}$ and hDHFR (HD). The flanking untranslated regions (5′U and 3′U), the location and orientation of primers (horizontal arrows), the restriction endonuclease sites (vertical arrows), and regulatory regions in the transfection construct (3′U of PvAC, 5′U of PyαTb, 3′U of PfHrp2) are indicated. **B.** Primers specific for different regions (5' integration, 5'-Int (1/2); 3' integration, 3'-Int (3/4); wild type locus, WTsp (1/4); vacuole membrane protein 1 gene as a control, Con) were used in PCR to differentiate the wild type and integration loci. PCR products for the indicated regions were amplified from the genomic DNAs of wild type (WT) and cloned knock-down (KD11 and KD9) parasites, and are shown in the ethidium bromide stained agarose gel. The lane M has DNA markers in kbps. **C.** The western blot of WT and knock-down (KD9 and KD11) parasite lysates was probed with antibodies to HA (ab-HA) or β-actin (ab-Ac).

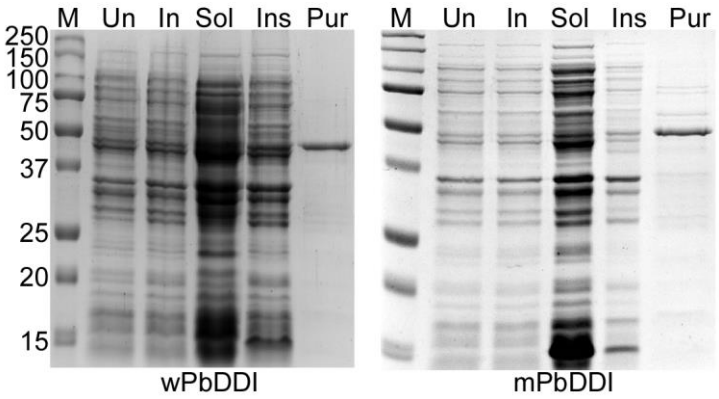

Figure S5. Production of recombinant PbDDI1. Wild type *P. berghei* DDI1 (wPbDDI) and its catalytic mutant (mPbDDI) were expressed as N-terminal His-taged proteins in BL21-CodonPlus (DE3) *E. coli* cells using the pRSET-A plasmid. The recombinant proteins were purified by Ni-NTA chromatography from IPTG-induced cells. The coomassie stained SDS PAGE gels show lysates of uninduced (Un) and induced (In) cells, soluble (Sol) and insoluble (Ins) fractions of induced cells, and Ni-NTA purified protein (Pur). The sizes of proteins markers (M) are indicated in kDa.

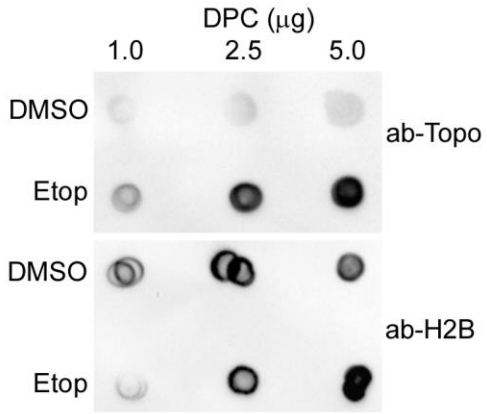

Figure S6. DPC preparation from HEK293T cells. DPCs were isolated from HEK293T cells treated with DMSO or etoposode (Etop). The indicated amounts of DPCs were spotted on a nitrocellulose membrane, and the presence of topoisomerase II-DPC was probed using anti-topoisomerase II antibodies (ab-Topo) antibodies. Antibodies to histone 2B were used as a control to ensure the presence of chromatin.

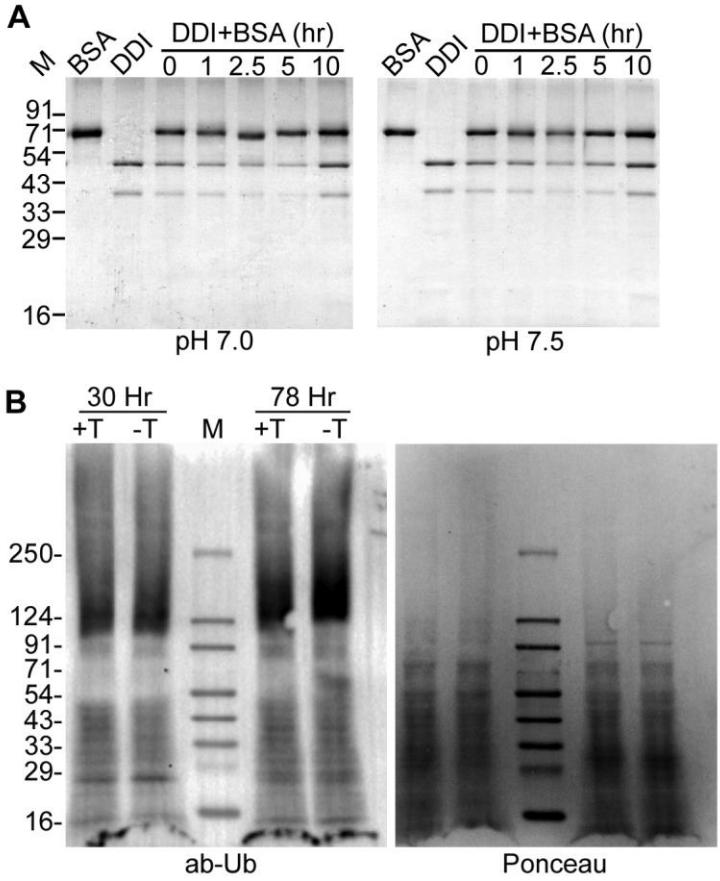

Figure S7. Protease activity of recombinant PfDDI. A. The reaction sample containing BSA and recombinant PfDDI1$_{Myc/His}$ (DDI+BSA) was incubated at 37°C, equal aliquots of the reaction sample were collected at the start and at the indicated time points, and the reaction was stopped with SDS-PAGE sample buffer. Control reaction samples contained BSA or DDI, incubated under identical conditions for 10 hours, and the reaction was stopped with SDS-PAGE sample buffer. The DDI+BSA aliquots, BSA and DDI1 samples were run in a 12% SDS PAGE and visualized by staining with coomassie blue. The intensity of BSA is similar across the incubation time points, indicating no degradation. The sizes of proteins markers (M) are in kDa. **B.** PfKD parasites were grown in the presence (+T) or absence (-T) of trimethoprim, harvested at 30 hr and 78 hr time points, and processed for the presence of ubiquitinated proteins by western blotting using anti-ubiquitin antibodies (ab-Ub). The membrane was stained with Ponceau before incubation with the blocking buffer, and shows similar loading of parasite lysates for the corresponding time point. The sizes of proteins markers (M) on the left margin of the blot are in kDa.

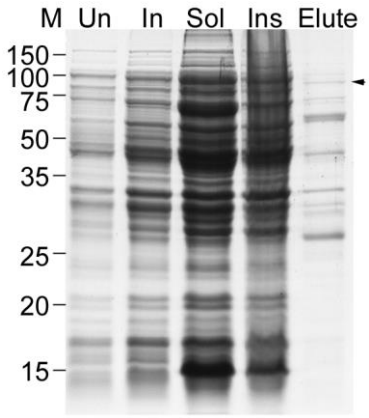

Figure S8. Production of recombinant PfPRP19. The PfPRP19 coding sequence was expressed with an N-terminal GST-tag in BL21-(DE3) *E. coli* cells using the pGEX-6P-1 plasmid and purified from the IPTG-induced cells. The coomassie stained SDS-PAGE gel show lysates of uninduced (Un) and induced (In) cells, soluble (Sol) and insoluble (Ins) fractions of the induced cells, and the GST-PfPRP19 enriched eluate (Elute). The arrow head indicates predicted size of GST-PfPRP19 (~87.7 kDa) and the sizes of proteins markers are indicated in kDa (M).

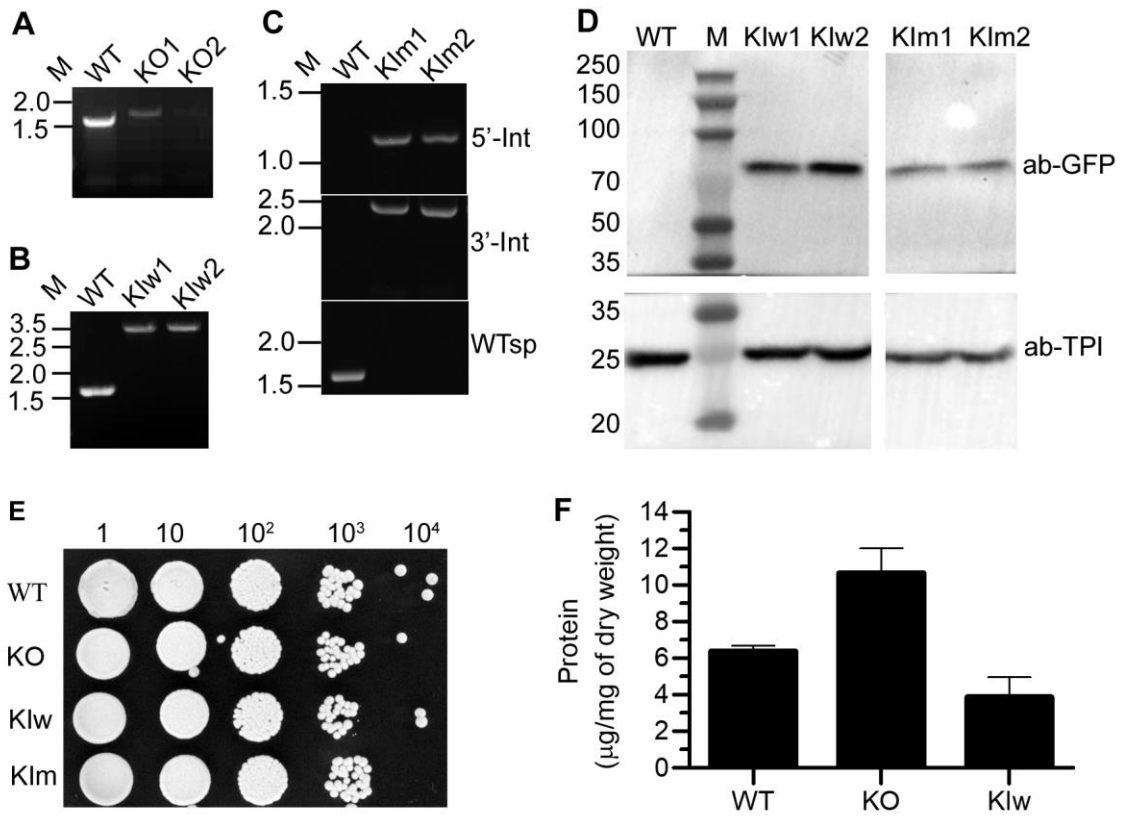

Figure S9. PfDDI1 reversed the hypersecretion phenotype of *S. cerevisiae* DDI1 mutant. The endogenous ScDDI was knocked-out (KO) by replacing the ScDDI1 coding region with a kanamycin cassette. For generation of complemented strains, the ScDDI1 coding region was replaced with GFP-wPfDDI/kanamycin cassette coding for wild type (KIw) or catalytic mutant (KIm) of PfDDI1. The replacement of ScDDI1 was confirmed by PCR of the gDNAs of wild type (WT), knockout (KO1 and KO2) and knock-in (KIw1, KIw2, KIm1 and KIm2) strains using locus-specific primers. **A and B.** The ethidium bromide stained agarose gels contains PCR products for the wild type (WT), knock-out (KO) and wild type PfDDI1-complemented (KIw) loci. **C.** The ethidium bromide stained agarose gel contains PCR products corresponding to the 5' integration (5'-Int), 3' Integration (3'-Int) and wild type-specific (WTsp) loci of WT and mutant PfDDI1-complemented (KIw) strains. The positions of DNA markers are in kbp (M). **D. Western blot analysis of complemented strains.** The lysates of WT, KIw and KIm strains were processed for western blott using anti-GFP antibodies (ab-GFP), and antibodies to triose phosphate isomerase antibodies (ab-TPI) were used as a loading control. The numbers indicate sizes of protein markers in kDa (M). **E. Comparative growth assay.** The overnight cultures of WT, KO, KIw and KIm strains were normalized to OD_{600} of 1.0, and the indicated dilutions of each culture were spotted on an YPD agar plate, which was incubated at 30°C till the colonies appeared. **F. Reversal of hypersecretion phenotype.** A single colony of each of the WT, KO and KIw strains was inoculated into SD medium and the cultures were grown for 48 hours at 30°C. The supernatant was dialyzed against PBS and the protein amount was estimated. The cell pellet was dried and weighted. The plot shows amount of protein in the supernatant normalized to the dry weight of cell pellet. The data is mean of three independent experiments with SD error bar.

Table S1. Primers used in the study.

Primer	Sequence (5'-3')
PfDdi-expF	ATGGGATCCGTTTTTATTACAATATCAGACGAT
PfDdi-expR	AATTAAAGCTTATAAATCATTGTTTGCATCAATGTC
PbDdiexpF	TATGGGATCCGTGTTCATAACAATATCTGATGAT
PbDdiexpRm	TAATAAGCTTCTACAGGTCTTCTTCAGAAATCAGCTTTTGTTCTAGTGTGTCTAAGTTTA TGTTTTC
Pbddimut-R	GTTTGTGCCCCTGAAGCGACAAATGCATG
PbDdimut-F	CATGCATTTGTCGCTTCAGGGGCACAAAC
PbDdiexpRm	TAATAAGCTTCTACAGGTCTTCTTCAGAAATCAGCTTTTGTTCTAGTGTGTCTAAGTTTA TGTTTTC
PRPsyn-Fchis	ATCGTACATATGGTGTTTATTACCATTAGCG
PRPsyn-Rchis	GAATTACTCGAGCAGATCCTCTTCGCTAATCAG
PbDdi1-Fl1F	AATTGCGGCCGCAAAAATTTCAATCATAGAGTATATATAC
PbDdi1-Fl1R	ATATGGTACCAGATCTCATTTTGGTCAAATCTTGTGATATTC
PbDdi1-Fl2F	ATAGCCTAGGGGCCCATAAAAATATACTATCCG
PbDdi1-Fl2R	AATTGGCGCCGGTTATTATTATCTTAAGTTTGTGACCATAC
DDiexp-F	ATGGGATCCGTTTTTATTACAATATCAGACGAT
DDimyc Rep-R	TAATCTCGAGTTACAGGTCTTCTTCAGAAATAAGCTTTTGTTCTAAATCATTGTTTGCAT CAATGTC
cDD-F	AATG*GGATCC*GGAGGCGGTGGAGGAATCAGTCTGATTGCGGCGTTA
cDD-R	CTAACTCGAGTCAAGCGTAATCTGGAACATCGTATGG
PfDdi-reF	AATGAGATCTGTTTTTATTACAATATCAGACGAT
PfDdi-cDDR	CCAAGGATCCCAGGTCTTCTTCAGAAATAAGCTTTTG
CON5'-F	GACAACATGATGCCCTTATGGAATATG
Pvac-R	CGGTCTGCAGCCCTGGAAAACAGGCGAT
Hrp2-F	ATCAGGCGCCATATCGAATTCCCGCGATCGATCCTAGGAACATATGTTTAAAAGAAAA ATTTAAGATTTACATGATTAGG
CON3'-R	CACTAAAATTCATAAGTGAAAAGTTGTCAC
Pbspec-F	CACATCAGCTACTAATGTTAGTACATCC
PFspec-F	TCTCTTAAATAATCCAGCTTTCAAAACA
α6FL2–F	ATAACCTAGGAGACGTGAAAGTTATATCGACC
α6FL2-R	AATTGATATCGAATTCCAAACACAAGCAAGCACTTGTGC
PfDDi3'U-F	TTATAGTCGACCGTAAATATTATTATCACTATCAATATATATGTAC
PfDDi3'U-R	AGCTTCTGCAGTTATTATTCATCTATTAACATAAGGGAAA
DDi-con5U	CTAACATTTTAACATTTTAATAATTAAGCATTAAAAATG
cDD-R	CTAACTGAGTCAAGGGTAATCTGGAACTCGTATGG
HRP2seq-F	CTTTTACAATATGAACATAAAGTACAAC
DDi3'int-R	CAACAGAATGTGCTCAGATCATAC
PfVMP1-Fep	TAGCTTAGATCTATGGATTCATATGAAGCTAAGAAGAAG
PfVMP1-R	CATTAGGTACCTTTTTTTATTTTTCTTGGTGTCATTTCGTTC
PfPPF19-Fexp	TAACGCAGATCTGGATCCATGTCAATAATATGCACCATAAGTGGC
PfPPF19-Rexp	GACTCTCGAGTTAGGTACCATTCCAAAGTTTTATTGTTTTATCCATTGA
ScDDi-Fko	GTATACTTAACGTAGTTAACAAAGTACATACCAAACATAACAGCAAAAATATACGTAA AGAGCGACATGGAGGCCCAGAATA
PfDDi-Rki	ACTTATCTATTTGTGTTATGGGCTACATACGTAGAGGCCGATCACAATATCAGTGGTTG CTCACAGTATAGCGACCAGCA
PRPsynD-A-F	GTGCATGCATTTGTTGCCAGCGGTGCACAGAGC
PfDDi-Rki	GCTCTGTGCACCGCTGGCAACAAATGCATGCAC
PfDDi-Fki	GTATACTTAACGTAGTTAACAAAGTACATACCAAACATAACAGCAAAAATATACGTAA AGATGAGTAAAGGAGAAGAACTTTTCAC
Sc/PfDDi-5con,	ATTCATCGCCACCGAAAAGATA
Sc/PfDDi-3con	TATACTTAACAGAAGTACAATC
RVP/UBA-F	TAAGTCAGCATATGGTTGTGTTCATGCTGTATATTCCGGTGGAA
PfDDIUbl-R	TACACTCACTCGAGTTAGTGATGGTGATGGTGATGTGCGCTGATTTTTTTGCGAACAAA

Table S2. Proteins identified in mass spectrometry analysis of the PfDDI1 immunoprecipitate. Shown are the score (Sc), coverage (Co), and number of unique peptides (UP) for each protein. The proteins shown were consistently identified in three independent biological replicates. The predicted pathway is based on homologs in other organisms.

Accession ID	Protein	Experiment 1			Experiment 2			Experiment 3			Pathway
		Sc	Co	UP	Sc	Co	UP	Sc	Co	UP	
Q8IM03 (PF3D7_1409300)	DNA damage-inducible protein 1	205.1	35.6	21	169.4	31.0	21	835.1	51.9	34	Bait protein
Q8I2Z8 (PF3D7_0915400)	Probable ATP-dependent 6-phosphofructokinase	144.1	24.6	26	12.1	2.7	4	15.8	5.1	6	Glycolysis pathway
Q8I3T1 (PF3D7_0517700)	Eukaryotic translation initiation factor 3 subunit B	123.6	36.5	22	9.9	4.3	3	5.7	1.4	1	Protein synthesis
O77325 (PF3D7_0308600)	Pre-mRNA-processing factor 19	60.8	20.3	8	10.2	6.4	3	12.1	7.7	2	DNA repair, mRNA splicing
Q8IKH8 (PF3D7_1465900)	40S ribosomal protein S3	46.4	41.2	8	20.7	27.6	7	73.6	38.0	9	Translation
O00806 (PF3D7_0309600)	60S acidic ribosomal protein P2	42.2	49.1	5	40.7	52.7	4	76.2	52.7	4	Translation
Q8IIA2 (PF3D7_1126200)	40S ribosomal protein S18	33.3	37.2	6	6.0	19.9	2	33.5	35.3	4	Translation
Q8I4Y9 (PF3D7_1244100)	N-alpha-acetyltransferase 15, NatA auxiliary subunit	31.8	8.2	8	3.4	1.2	1	1.7	1.8	1	-
Q8IAX6 (PF3D7_0814000)	60S ribosomal protein L13	30.6	24.7	6	16.3	19.5	4	51.8	22.8	6	Translation
Q8IAL3 (PF3D7_0801500)	Nucleolar protein 10	28.8	16.0	7	31.4	12.8	6	35.1	17.5	8	-
Q8ILK3 (PF3D7_1426000)	60S ribosomal protein L21	26.1	38.5	5	4.1	10.6	1	44.0	35.4	6	Translation
Q8IM23 (PF3D7_1407100)	Fibrillarin	25.1	22.6	7	11.9	12.3	4	40.7	31.8	8	rRNA processing
C0H5C2 (PF3D7_1317800)	40S ribosomal protein S19	25.1	22.8	3	7.9	18.6	2	44.2	36.6	5	Translation
Q8IHT2 (PF3D7_1143400)	Translation initiation factor eIF-4C	24.5	28.4	4	8.2	11.0	2	11.0	16.8	2	Translation
Q8IKS3 (PF3D7_1455500)	AP-1 complex subunit gamma	22.9	7.2	6	2.2	1.3	1	14.8	4.3	3	-
Q8I0W8 (PF3D7_0513600)	Deoxyribodipyrimidine photo-lyase	22.2	6.7	6	9.0	3.2	3	8.9	1.8	2	-
Q7K6A0 (PF3D7_0934800)	cAMP-dependent protein kinase catalytic subunit	21.3	24.0	8	3.7	7.3	3	6.6	7.6	2	Signal transduction
Q8I5C4 (PF3D7_1229500)	T-complex protein 1 subunit gamma	21.1	15.5	8	22.8	12.9	6	41.1	14.9	7	Protein folding
P50250 (PF3D7_0520900)	Adenosylhomocysteinase	19.6	18.0	8	12.3	8.6	4	56.1	22.3	10	Amino-acid biosynthesis
O96220 (PF3D7_0214000)	T-complex protein 1 subunit theta	19.5	11.8	7	13.3	9.6	5	33.1	13.7	7	-
Q8I2B1 (PF3D7_0102900)	Aspartate--tRNA ligase	19.4	7.4	5	18.3	6.7	4	23.3	10.4	6	-
C6KT23 (PF3D7_0618300)	60S ribosomal protein L27a	18.7	31.8	5	4.8	6.8	1	8.6	23.0	3	Translation
Q8I577 (PF3D7_1234500)	Uncharacterized protein	16.1	14.3	5	4.3	2.9	1	29.4	18.5	6	-
Q8ILY9 (PF3D7_1410600)	Eukaryotic translation initiation factor 2 gamma subunit, putative	16.1	9.0	4	16.4	12.0	5	19.1	10.5	3	Translation
Q8I3R6 (PF3D7_0519400)	40S ribosomal protein S24	15.4	31.6	5	5.7	18.1	2	24.0	15.8	4	Translation
O77381 (PF3D7_0317600)	40S ribosomal protein S11	12.8	26.7	4	32.5	37.9	6	46.9	41.0	7	Translation
Q8I3R0 (PF3D7_0520000)	40S ribosomal protein S9	11.6	16.9	4	13.3	18.5	4	42.4	28.0	6	Translation

Q8IDR9 (PF3D7_1342000)	40S ribosomal protein S6	10.6	16.3	3	4.9	10.8	2	38.9	19.9	6	Translation
C6KT56 (PF3D7_0621900)	Signal recognition particle subunit SRP68	10.3	4.0	4	15.1	6.6	5	47.6	12.0	10	Translation
Q8IIB4 (PF3D7_1124900)	60S ribosomal protein L35	10.2	27.4	4	6.7	6.5	2	23.6	21.0	4	Translation
Q8IBH7 (PF3D7_0728000)	Eukaryotic translation initiation factor 2 subunit alpha	9.1	11.6	4	12.5	14.3	4	6.2	3.7	1	Translation
Q8IKU0 (PF3D7_1453800)	Bifunctional glucose-6-phosphate 1-dehydrogenase/6-phosphogluconolactonase	9.1	5.3	5	17.0	6.3	5	33.5	7.7	6	-
Q8I5X9 (PF3D7_1206600)	DNA-directed RNA polymerase subunit beta	8.2	2.6	4	42.9	9.4	12	54.4	9.2	11	Transcription
Q8IJT9 (PF3D7_1010600)	Eukaryotic translation initiation factor 2 subunit beta	7.6	12.6	3	5.2	5.4	1	15.6	17.6	4	Translation
O77364 (PF3D7_0312800)	60S ribosomal protein L26	7.1	7.1	1	3.6	7.1	1	7.8	7.1	1	Translation
Q8I3X4 (PF3D7_0513300)	Purine nucleoside phosphorylase	6.0	10.6	2	4.8	8.6	2	29.2	24.5	4	-
Q8IJV5 (PF3D7_1009000)	Diphthine methyl ester synthase	5.3	9.1	2	1.7	2.6	1	1.7	2.6	1	-
Q8IKQ7 (PF3D7_1457300)	MA3 domain-containing protein	4.8	2.8	2	2.3	2.5	2	25.8	5.8	3	-
Q8ILW6 (PF3D7_1412800)	Glycylpeptide N-tetradecanoyltransferase	4.8	3.9	1	4.8	4.9	2	0.0	1.7	1	-
Q8ID96 (PF3D7_1361000)	Protein arginine N-methyltransferase	4.7	1.9	1	2.1	1.9	1	11.0	1.9	1	-
C0H5D7 (PF3D7_1326400)	Translation initiation factor eIF-2B subunit gamma	4.0	1.9	1	7.7	5.7	3	8.2	3.4	2	Translation
Q8ID33 (PF3D7_1367500)	NADH-cytochrome b5 reductase	4.0	4.4	2	3.4	4.7	2	3.9	2.5	1	-
C6KT96 (PF3D7_0626000)	Uncharacterized protein	3.0	1.4	2	10.3	1.8	3	6.3	1.4	2	-
Q8IEM3 (PF3D7_1309100)	60S ribosomal protein L24	3.0	6.8	1	3.8	11.7	2	6.6	11.1	2	Translation
Q8ILP6 (PF3D7_1420400)	Glycine--tRNA ligase, dATP synthetase	2.8	1.6	1	2.1	0.9	1	0.0	0.8	1	-
Q8IEP9 (PF3D7_1306600)	V-type proton ATPase subunit H	2.7	2.9	1	1.6	1.5	1	5.1	3.1	1	-
C0H4Y0 (PF3D7_0826500)	Ubiquitin conjugation factor E4 B	2.3	0.9	1	7.4	1.4	2	6.2	1.9	2	UPS
Q8I5F9 (PF3D7_1225800)	Ubiquitin-activating enzyme E1	2.2	1.3	1	2.8	2.2	2	3.9	3.7	2	UPS
C0H5B3 (PF3D7_1313800)	Uncharacterized protein	2.2	0.4	1	1.9	0.5	2	0.0	0.3	1	-
Q8IIU6 (PF3D7_1105700)	tRNA-splicing ligase RtcB homolog	2.1	3.6	2	0.0	2.0	1	7.0	5.1	2	-
C0H4K8 (PF3D7_0705700)	40S ribosomal protein S29	2.1	13.0	1	1.8	13.0	1	5.4	14.8	1	Translation
O96185 (PFB0460c)	Uncharacterized protein	2.0	0.4	1	2.8	0.5	1	15.7	2.5	4	-
Q8IJV3 (PF3D7_1009200)	Small subunit rRNA synthesis-associated protein	1.9	1.1	1	6.0	2.5	2	4.1	0.8	1	-
O77323 (PF3D7_0308200)	T-complex protein 1 subunit eta	1.9	3.2	1	9.6	5.2	2	21.5	8.5	4	Protein folding
Q8IHY0 (PF3D7_1138500)	Protein phosphatase PPM2	1.9	1.0	1	4.6	1.0	1	3.2	1.5	1	-
Q8IBB6 (PF3D7_0828500)	Translation initiation factor eIF-2B subunit alpha	1.9	2.9	1	3.0	4.1	1	18.5	14.9	3	Translation
C6KTB3 (PF3D7_0627700)	Transportin	1.7	1.0	1	2.0	0.8	1	3.1	1.0	1	Protein import into nucleus
C0H489 (PF3D7_0405100)	Protein transport protein Sec24B	1.6	0.7	1	3.1	1.0	1	12.9	3.3	3	Protein transport

Q8IHU0 (PF3D7_1142500)	60S ribosomal protein L28	0.0	15.8	2	8.4	22.8	3	16.5	15.8	2	Translation
Q8IBI3 (PF3D7_0727400)	Proteasome subunit alpha type	0.0	3.9	1	2.0	3.1	1	8.3	6.3	1	UPS
C6KTE1 (PF3D7_0630600)	DUF4205 domain-containing protein	0.0	2.3	2	7.8	2.8	2	18.5	7.2	6	UPS
Q8I5E0 (PF3D7_1227800)	Histone S-adenosyl methyltransferase	0.0	0.9	1	5.3	1.8	2	2.4	1.9	1	-